Université d'Ottawa · University of Ottawa

Université d'Ottawa · University of Ottawa

FACULTÉ DES ÉTUDES SUPÉRIEURES ET POSTDOCTORALES

FACULTY OF GRADUATE AND POSTDOCTORAL STUDIES

Darren John PORTER

AUTEUR DE LA THÈSE - AUTHOR OF THESIS

M. Sc. (Chemistry / Spec.: Chemical and Environmental Toxicology

GRADE - DEGREE

Department of Chemistry

FACULTÉ, ÉCOLE, DÉPARTEMENT - FACULTY, SCHOOL, DEPARTMENT

TITRE DE LA THÈSE - TITLE OF THE THESIS

Analysis of Oil Resins Using Electrospray Inonization Mass Spectrometry

P. Mayer

DIRECTEUR DE LA THÈSE - THESIS SUPERVISOR

CO-DIRECTEUR DE LA THÈSE - THESIS CO-SUPERVISOR

EXAMINATEURS DE LA THÈSE - THESIS EXAMINERS

J. Giorgi

E. Lai

J.-M. De Koninck, Ph.D.

LE DOYEN DE LA FACULTÉ DES ÉTUDES SUPÉRIEURES ET POSTDOCTORALES

SIGNATURE

DEAN OF THE FACULTY OF GRADUATE AND POSTDOCTORAL STUDIES

Analysis of Oil Resins Using Electrospray Ionization Mass Spectrometry

Darren J. Porter

Thesis submitted to the Faculty of Graduate & Postdoctoral Studies
University of Ottawa
In partial fulfillment for the requirements for
Masters in Chemical and Environmental Toxicology

Ottawa-Carleton Institute of Chemistry

July 2003

Candidate	Supervisor
Darren J. Porter	Paul M. Mayer

Your file Votre référence
ISBN: 0-612-90345-1
Our file Notre référence
ISBN: 0-612-90345-1

Abstract

Each year there are accidents involving oil tankers, pipelines, and storage facilities resulting in the release of large quantities of oil into the environment. As a result, oils are usually characterized for identification purposes. Nitrogen-containing aromatic compounds (NCACs) such as substituted pyridines, indoles, quinolines and carbazoles are known to occur in the low to high molecular weight fractions of crude oil. Use of the popular SARA fractionation procedure allows oils to be separated into fractions containing Saturates, Aromatics, Resins, and Asphaltenes. This allows for the individual and chemical class identification of many of the constituents present in oils worldwide. The objective of this research was to use Electrospray Ionization Tandem Mass Spectrometry (ESI-MS/MS) to study a variety of NCACs for use in the analysis of the Resins fraction of several crude oils. In addition, the affect of weathering on these oil resins was studied using a technique employing Electrospray Ionization Mass Spectrometry (ESI-MS).

Acknowledgements

This thesis was prepared under the advisorship of Dr. Paul M. Mayer. His guidance, advice, and knowledge of mass spectrometry made this an enjoyable experience, and are highly appreciated.

Thanks to Dr. Mervin Fingas, Dr. Zendi Wang, and Dr. Bruce Hollebone at the Emergencies Science Division of Environment Canada for providing the heterocycles and resin extracts that were used for this work.

I would also like to thank Dr. Clement W. Kazakoff at the Mass Spectrometry Centre for conducting the GC-MS analysis of the heterocycles.

To my son Alexander and to my

wife Delphine for her support and

encouragement during this

endeavour.

Table of Contents

List of Figures

List of Tables

List of Acronyms and Abbreviations

AMU	Atomic Mass Unit
ASMB	Alberta Sweet Mixed Blend
BTEX	Benzene, Toluene, Ethylbenzene, and Xylene
CI-MS	Chemical Ionization Mass Spectrometry
CID	Collision-Induced Dissociation
ESI-MS/MS	Electrospray Ionization Tandem Mass Spectrometry
ESI-MS	Electrospray Ionization Mass Spectrometry
FID	Flame Ionization Detection
FTIR	Fourier Transform Infrared
GC	Gas Chromatography
GC-MS	Gas Chromatography-Mass Spectrometry
HFO	Heavy Fuel Oil
HPLC	High-Performance Liquid Chromatography
IR	Infrared
LEC	Ligand Exchange Chromatography
MIKE	Mass analyzed Ion Kinetic Energy
Mn	Number Average Molecular Weight
MS	Mass Spectrometry
m/z	Mass to Charge
NCAC	Nitrogen Containing Aromatic Compounds
NMR	Nuclear Magnetic Resonance
NNC	Neutral Nitrogen Compounds
NPAH	Nitrogen Poly-Aromatic Hydrocarbons
PAC	Polar Aminocyano
PAHs	Polycyclic Aromatic Hydrocarbons
RF	Radio Frequency
SARA	Saturates, Aromatics, Resins, and Asphaltenes
SFC	Supercritical Fluid Chromatography
SIM	Selected-Ion Monitoring
UV	Ultraviolet
XANES	X-ray Absorption Near-Edge Structure

Chapter 1 - Introduction

Consumer and industrial demand for petroleum products has lead to the mass transport of bulk crude oil all over the world. Each year there are accidents involving oil tankers, pipelines, and storage facilities resulting in the release of large quantities of oil into the environment. Movement of petroleum from the oil field to the consumer may require 10 to 15 transfers between as many as six different transportation modes, including tankers, pipelines, trains, and tank trucks, as well as temporary storage in a variety of facilities [1]. With so many different transfers, the probability of spills during one or more of these avenues is quite high. Spills, whether deliberate or unintentional are the major source of oil introduction into freshwater and salt-water environments. Moriarity [2] compiled a list of the sources and estimated amounts of crude oil and its products released into the marine environment. Incidents related to the transport of oil accounted for 25% of all spills with bilge water and fuel oil releases being the highest in that category at 252 kilotonnes per year. Tanker operation (washing-out tanks) and accidents with tankers were the next highest at 158 and 121 kilotonnes, respectively. The highest reported source of spills was from municipal and industrial wastes and surface run off at 1060 kilotonnes per year. Estimated total oil and oil products spilled per year is 2365 kilotonnes. When compared to the annual world production of crude oil of about 3×10^6 kilotonnes, this equates to less than 0.1% of all produced oil being spilled into the environment. Once spilled, oil can impact many different organisms in both the terrestrial and aquatic environments. The well-publicized

aftermath of various oil spills has heightened public awareness of the effects and the damage caused to the environment.

Petroleum is a naturally occurring high hydrocarbon mixture that is usually obtained from below the earth's surface. In fact, hydrocarbons constitute about 50-90% of petroleum while the remainder is composed chiefly of organic compounds containing O, N, S, and trace amounts of organometallic compounds [3]. The hydrocarbons can be grouped into four major classes according to their general composition: (1) saturates, (2) aromatics, (3) resins and (4) asphaltenes. The saturates contain alkanes and cycloparaffins that range from methane to n-hexacontane ($C_{60}H_{122}$). The aromatics include mono-, di-, and polycyclic aromatic hydrocarbons (PAHs). Resins contain aggregates with a multitude of building blocks like sulfoxides, amides, thiophenes, pyridines, quinolines, and carbazoles. Asphaltenes consist of aggregates of extended polyaromatics, naphthenic acids, sulfides, polyhydric phenols, fatty acids, and metallophorphyrins. Heterocyclic nitrogen-containing compounds comprise the neutral or basic fraction of crude oil. Pyrroles and derivatives such as indoles and carbazoles dominate the neutral fraction while the basic fraction consists mainly of pyridines and their derivatives such as quinolines, benzoquinolines, and acridines [4]. In general, the composition of an oil can vary greatly depending on the source.

Petroleum oils are toxic to a wide range of life forms, from unicellular organisms to plants and vertebrates. Various oil constituents can induce toxicity in fish and birds, two major

sufferers of ocean spilled oil. As well, spilled oil can remain on oceans and coastlines indefinitely until degraded by weathering processes. Aromatic hydrocarbons have been identified as the main class of compounds in crude oils with the greatest toxic effects. They include compounds like naphthalene, phenanthrene, quinoline, acridine, and phenols. Black *et al.* [5] found that chemicals in this class exhibited 96 hour LC50s in the range 0.04-11.0 mg/L when exposed to embryo-larval stages of rainbow trout and largemouth bass. It was noted that for each class of compounds, the chemical with the greater number of aromatic rings always exerted the greater toxicity. In addition, teratogenic deformities were seen in 6% of embryos of largemouth bass after seven-day exposures to naphthalene at a concentration of 0.24 mg/L. The toxicity of an artificial mixture of 18 PAHs was tested on embryos of chicken, turkey, mallard duck, and common eider at doses of 2.0 mg/kg and 0.2 mg/kg of egg [6]. Mortality was significantly increased in all four birds at the higher dose and in mallards at the lower dose. However, when the 18 compounds were tested individually, only benzo[k]fluoranthene, benzo[a]pyrene, and indenopyrene caused significant increases in mortality of chicken embryos at the higher dose. There is a vast amount of published work on the ecotoxicological effects of PAHs on aquatic organisms indicating that variations in experimental conditions can produce different results [7].

The frequent occurrence of oil spills and the persistence of oil in the environment have lead to the need for scientists to be able to analyze oil so it can be effectively tracked in the environment. In order to do this, researchers have been developing methods to monitor the fate and behaviour of spilled oil. Some of these methods have also been applied in the study of the effects of oil on aquatic and terrestrial organisms. The present review covers the techniques that

have been used for analyzing crude oil and its various fractions. It also covers research conducted to monitor the weathering process of crude oil.

1.1 Separation and Analysis Schemes for Crude Oil

1.1.1 Liquid Chromatography Separation

Crude oil is such a complex mixture that a complete separation of all constituents would be difficult, if not impossible. As a result, researchers have focused on separating various fractions or classes of chemicals from oils. This has allowed for the determination of many different components in oil and provided a somewhat better understanding of its composition. When performing chemical measurements of spilled oil, the main objectives are generally considered to be : (1) to identify and quantify the major individual components and compound classes which are useful for study of oil fate and behaviour in the environment; (2) to identify and quantify the environmentally hazardous constituents; and (3) to characterize marker compounds which can be reliably used to indicate source, nature and type of the spilled oils and to differentiate the petroleum products from background pollution sources in the samples [8]. Marker compounds, usually referred to as biomarkers, can be used to fingerprint oil and track its fate. The term "biomarker" is used by scientists to reflect the fact that crude oil is the result of the breakdown of biological substances of plant, animal or mineral origin.

The techniques most commonly used today for oil analysis include gas chromatography (GC), gas chromatography-mass spectrometry (GC-MS), high-performance liquid chromatography (HPLC), infrared spectroscopy (IR), supercritical fluid chromatography (SFC), ultraviolet (UV) and fluorescence spectroscopy, and nuclear magnetic resonance (NMR). Of all these techniques, high-resolution capillary GC with flame ionization detection (FID) and combination of capillary GC with other techniques such as GC-MS are the most widely used [9]. Methods employing UV or IR for the analysis of oil have so far only been able to provide estimates of whole fractions present.

Many schemes have been developed to separate the neutral and basic fractions of oil including the very popular SARA method (Saturates, Aromatics, Resins, and Asphaltenes). This approach is based on the adsorption of the sample on either silica or alumina followed by selective elution of the constituents using a series of increasingly polar solvents [3]. The petroleum fractions can then be analyzed using selective analytical techniques like those mentioned previously. Ali *et al.* [10] separated an Arabian heavy crude oil residue by alumina chromatography into saturates (18.2%), aromatics (52.4%), resins (17.8%), and asphaltenes (11.6%) using the SARA method. Characterization of the asphaltene fraction revealed that it was hydrogen deficient, indicating a high degree of ring condensation. The resin fraction had 4.9% oxygen content and was found to contain carboxylic acids, phenols, and other oxy compounds.

In the literature, several liquid chromatography separation schemes for different chemical classes in oil have been proposed. Akhlaq [11] used a HPLC backflush method to separate crude

oils, fuel oils, and other related products into aliphatics, one-, two-, and three ringed aromatics, polar compounds, resins, and asphaltenes. The procedure was able to separate oils and middle distillates into seven fractions suitable for analysis by GC-MS. The process made use of a Bondapak NH_2 column through which all but the polar compounds (NH-, SH- and OH-substituted) and colloids (resins, and asphaltenes) were passed. Then the column was backflushed resulting in elution of the latter two groups.

A more recent process used by Rudzinski and Aminabhavi [3] involved the separation of sulfur containing compounds in the saturate and aromatic fractions of Maya crude oil. These fractions were separated using ligand exchange chromatography (LEC), a process which relies on the organosulfur affinity for Cu^{2+} and Pd^{2+}. Structural characterization was then performed using elemental analysis, FTIR (Fourier Transform Infrared) and NMR. Supercritical fluid chromatography, which employs a supercritical fluid as the mobile phase, originated with high-pressure gas chromatography. This method is a high-resolution separation technique suitable for the analysis of organic compounds that are nonvolatile, polar, thermally labile, or of high molecular mass [3]. SFC uses gases like carbon dioxide, ethane, propane and toluene, or a simple liquid like water at operating temperature and pressure just above the critical values. As a result, the supercritical fluid has a density and dissolving ability similar to a liquid and diffusivity, viscosity, and surface tension similar to a gas. In chromatography applications, this can lead to greater selectivity, rapid mass transfer, and high flow rates when compared to liquids. Rudzinski and Aminabhavi [3] conducted a review of SFC applications for crude oil analysis. They reported

many different applications of this methodology, most of which employed supercritical carbon dioxide to extract aromatics, alkanes, and other oil constituents for further analysis.

A comparison of normal-phase and reverse-phase high-performance liquid chromatography for the separation of polycyclic aromatic hydrocarbons and nitrogen heterocycle compounds in solvent refined coal liquids was completed by Ruckmick and Hurtubise [12]. For normal-phase, the columns studied were μPorasil, Nucleosil NO_2, basic alumina, μBondapak NH_2, and μBondapak CN. The reverse-phase columns tested were μBondapak C18 and μBondapak CN. Only the μPorasil column was able to resolve polycyclic aromatic hydrocarbons from the nitrogen heterocycles under normal-phase conditions. However, both columns used in the reverse-phase study were able to resolve these two functional classes. It was noted that the solubility of solvent refined coal liquids in reverse-phase systems limits the usefulness of this approach.

Frolov [13] reported a method for isolating petroleum carbazole concentrates based on liquid chromatography on silica gel. Separation of a total carbazole concentrate into C1, C2, C3 and C4 subfractions was achieved using a C18 column and elution with CH_3CN/H_2O (7:3). Reverse-phase HPLC separation of petroleum carbazoles was governed only by the number of carbon atoms in the molecule, and was without structural selectivity. Separation of triaromatic nitrogen bases in crude oils has also been achieved using a C18 column [14]. In this work, the authors used an analytical sequence which involved the trapping of strong nitrogen bases on HCl

modified silica followed by purification using reverse-phase HPLC. Fractions containing triaromatic azaarenes with two to seven fused rings were obtained using this method. These fractions were then analyzed using UV spectra enabling a determination of the location of the nitrogen atom in the petroleum triaromatic azaarenes.

Snyder and Buell [15] developed a general separation scheme for nitrogen and oxygen compound types in petroleum. Cation and anion exchange were used in conjunction with adsorption chromatography on alumina, silica, and charcoal. An integrated separation scheme based on these individual procedures was assembled. Application of this scheme to a 700-850 °F petroleum distillate resulted in recovery of 96% nitrogen, 115% oxygen, 96% weak acids, and 104% weak bases [16]. Major compound types (>0.1% wt) included indoles, carbazoles, benzocarbazoles, pyridines, quinolines, phenanthridines, hydroxypyridines, hydroxyquinolines, dibenzofurans, naphthobenzofurans, phenols, aliphatic ketones, carboxylic acids, and sulfoxides.

Several liquid chromatographic separation schemes for petroleum compounds using alumina have been reported in literature. Mao *et al.* [17] developed a methodology for the analysis of neutral nitrogen compounds in diesel oil by normal phase HPLC. The diesel oils were diluted with one volume of hexane and injected directly onto an alumina analytical column. Non-basic nitrogen compounds were eluted using a gradient hexane/dioxane mobile phase revealing alkylcarbazoles and alkylindoles as the major components. However, the method was not applicable to basic nitrogen compounds because of their high polarities. A method for effectively separating synthetic fuels was described by Later *et al.* [18]. Prefractionation of crude synfuel

materials from a solvent-refined coal liquid was achieved using neutral alumina oxide and silicic acid in an adsorption chromatography procedure. The chemical classes investigated were aliphatic hydrocarbons, polycyclic aromatic hydrocarbons, polycyclic aromatic sulfur heterocycles, nitrogen polycyclic aromatics, and hydroxyl polycyclic aromatic hydrocarbons. Schiller and Mathiason [19] reported the development of a chromatographic procedure using neutral alumina to fractionate a wide variety of coal-derived solids and liquids. The method allowed for the separation of saturated hydrocarbons, aromatic hydrocarbons, benzofurans, ethers, nitrogen compounds, and hydroxyl compounds. Basic and neutral alumina were used by Ford et al. [20] to separate nitrogen compounds in hydrotreated shale oil using adsorption chromatography. Analysis of the fractions by infrared spectrometry revealed three major nitrogen compound types: pyridine-type nitrogen, pyrrole-type nitrogen, and amide-type nitrogen.

Application of a polar aminocyano-bonded silica column (PAC) for the rapid separation of pyrrole and pyridine nitrogen heterocycles has been reported by Li *et al.* [21]. The new separation scheme made it possible to identify the isomeric nitrogen compounds, particularly the pyrrole nitrogen species. The method was successful in the separation of nitrogen heterocycles from light whole oils with nitrogen contents as low as 0.1 wt%.

1.1.2 Analysis of Crude Oil by Mass Spectrometry

Mass spectrometry allows for the easy identification and quantification of individual components in crude oil fractions. Chemical classes like indoles, carbazoles, and quinolines are easily identified using MS. Stefanova *et al.* [22] obtained homogeneous fractions of carbazoles, benzocarbazoles, and their alkyl derivatives after extensive chromatographic separation. The study, which focused on neutral nitrogen compounds (NNC), indicated that the number and position of alkyl substituents could be determined by ^{1}H NMR and electron-impact mass spectrometry.

According to Wang *et al.* [23], high-resolution capillary GC equipped with flame ionization detection and capillary GC-MS are the most important and widely used techniques for oil separation, characterization, and identification. These authors have used GC-MS extensively for the identification of oil and petroleum type products on numerous occasions [23-29]. In each case, the mass spectrometer was operated in the scan and selected-ion monitoring (SIM) modes to obtain data for the identification of the components, and in the SIM mode for quantitation of target compounds. SIM mode involves monitoring preselected ions which are useful for identifying, characterizing, and quantifying the oil components of interest. Operating in SIM mode provides several distinct advantages: 1) the detection limits are generally lower by almost an order of magnitude than for full scan GC-MS; 2) sensitivity of the instrument is increased while operating in this mode thereby lowering the detection limit; and 3) increased linear range of the instrument for low-concentration analytes. By means of MS-SIM, the authors have

identified and quantified aliphatics and aromatics [23], and the well known benzene, toluene, ethylbenzene, and xylene (BTEX) components in crude oil [25].

An identification of non-basic nitrogen containing polyaromatic hydrocarbons (NPAHs) in hydrotreated coker gas oil using MS has been reported by Ignatiadis *et al.* [30]. Six crude oils of different origin and geological history were tested for carbazole content. The non-basic compounds identified as alkylbenzocarbazoles and alkylcarbazoles were found to be rare.

Brumley *et al.* [31] were able to characterize nitrogen containing aromatic compounds (NCACs) in soil and sediment using full-scan electron ionization MS. Isolation and quantitation of NCACs was achieved using a two-step fractionation scheme based on acid-base partitioning of basic compounds and preparative TLC isolation of neutral compounds. Guan and Marshall [32] were able to resolve ions in the low-voltage electron impact mass spectrum of the aromatic neutral fraction of gas oil. This was achieved using a Fourier transform ion cyclotron resonance (FT-ICR) mass spectrometer. Fourier transform mass spectrometry is a technique in which mass analysis is performed by detecting the cyclotron frequencies of ions (i.e., the cyclic motion of ions in a magnetic field). The authors compared their results with those generated using a double-focusing mass spectrometer. They concluded that FT-ICR/MS provided the best available mass resolution and mass accuracy for molecular ion type analysis of aromatic neutral gas oil.

Recently, Zhan and Fenn [33] used electrospray ionization mass spectrometry (ESI-MS) for the analysis of fossil fuels. In ESI-MS, ions present in solution can be transferred to the gas

phase for subsequent analysis by a mass spectrometer. Electrospray results in the dispersion of cations and anions into tiny charged droplets through the application of an intense electric field [34]. The method works well for polar compounds with a permanent dipole. However, the analysis of non-polar type compounds commonly found in crude oil has proved difficult using ESI. The above authors carried out exploratory experiments on crude oil, jet fuel, gasoline, and coal to test the applicability of this identification process. Two types of heavy crude oil, "Alba" from the North Sea Basin and "Maya" from a major oil field in Mexico were analyzed as well as the asphaltene fraction of one of the oils. The spectra contained a substantial amount of information on the composition and character of these materials. The "difference spectrum" for each oil revealed that the distribution of polar species is a unique characteristic or "fingerprint" by which the crude can be identified. As a result of this work it appears that ESI-MS may find application in tracing the source of spilled oils.

1.1.3 Monitoring the Oil Weathering Process

After oil is spilled on land or into the ocean it is immediately subjected to several weathering processes that include evaporation, dissolution, dispersion, photochemical oxidation, water-oil emulsification, microbial degradation and adsorption onto suspended particulate materials [8]. The degradation can produce a variety of substrates for various indigenous microbial groups. Lightly weathered oils suffer from loss of n-alkanes; moderately degraded oils show a heavy loss of n-alkanes and a partial loss of lighter polycyclic aromatic hydrocarbon

compounds. In heavily degraded oils, the n-alkanes and branched alkanes could be completely lost, and PAHs could be highly degraded.

Volatilization can result in loss of up to 75% of light crude oil, 40% of medium, and 5-10% of heavy and residual oil in the first few days following an oil spill [29]. The rate of evaporation depends on the volatility of individual components present in the oil. It is also affected by environmental factors like air and water temperature, water turbulence, and wind. Other degradation processes act over a longer period to disperse and remove as much as possible of the remaining oil fractions. Dissolution usually involves loss of components to the water surrounding an oil slick. However, most of the components of oil are hydrocarbon based and have a very low solubility in fresh or salt-water. Some sulfur compounds and salts present in the oil would be good candidates for the dissolution process. Unlike evaporation, dissolution continues long after an oil spill because oxidation and microbial degradation result in the production of more soluble compounds. Oxidation is slow compared to evaporation and only occurs at the surface of an oil slick. The rate of oxidation can be increased by mineral salts and by metals like vanadium that act as catalysts in the oxidation process. The rate of biodegradation due to microbial action on oil can be as high as 2 grams of oil per square meter per day [1]. This type of degradation is dependent on the temperature of the oil and water mixture, with more efficient degradation occurring at higher temperatures in well-oxygenated waters.

Wang and Fingas [9] have summarized the major compositional changes of aromatics in oil due to weathering as follows: (1) the degradation rates are correlated to molecular mass, boiling points and degree of alkylation of the aromatic compounds; (2) the degradation rates of PAHs are proportional to the number of aromatic rings; (3) degradation rates are inversely proportional to the degree of alkylation of the benzene and PAH homologues; and (4) of the five alkylated PAH homolog families, the alkylated chrysenes series is the least susceptible to weathering as indicated by the increase of their percentages in the total of the alkylated PAHs and the relative decrease in the ratios of the sum of naphthalenes, phenanthrenes, dibenzothiophenes and fluorenes to the sum of chrysenes.

Establishing a fingerprint for oil and measuring the degree to which it is degraded over time is frequently accomplished using biomarker compounds. Petroleum geochemists have used triterpanes and steranes for decades to identify oils while chemists have more recently been using them to study the fate of spilled oil. According to Wang *et al.* [24] the analysis of biomarker compounds offers several advantages: 1) triterpanes and steranes are unique for each oil and have distinct distribution patterns; 2) they are highly degradation resistant compounds in comparison to aliphatic and aromatic compounds; and 3) calculations based on hopane analysis to estimate percent of oil depletion can provide a more accurate representation of the degree of oil degradation than the traditional aliphatic/isoprenoid hydrocarbon ratio, and can greatly improve the ability to resolve biodegradation differences between sites.

Biodegradation of the hydrocarbon constituents in oil is dependent on type of bacteria, temperature and the nature of the oil. The ability of microrganisms to change the chemical composition of oil has been studied quite extensively over the last ten or more years and researchers now have a better understanding of the process. Early investigations of microbial degradation focused on n-alkanes followed by aromatic compounds and later sulfur heterocycles. Fedorak *et al.* [35] studied the effect of microbial degradation of nitrogen heterocycles in crude oil. An oil-degrading mixed bacteria culture was enriched with carbazole to enhance its ability to degrade nitrogen heterocycles. The bacteria degraded most of the C1-, C2-, and C3- carbazoles and one of the C4- isomers within 8 days. Dutta and Harayama [36] investigated the effect of bacterial and photooxidation biodegradation of long-side-chain alkylaromatics in Arabian light crude oil in order to evaluate the fate of these compounds in the environment. The n-alkylbenzenes were found to be quite susceptible to biodegradation (86.3% ave) but not photooxidation (5.3% ave), whereas the n-alkylbenzothiophenes were almost completely photooxidized (94.8% ave) and substantially degraded (78% ave).

Page *et al.* [37] studied the weathering process of several oils that were spilled off the coast of Brittany, France. Sediment hydrocarbon analyses were performed to generate data allowing conclusions to be drawn concerning the source of the hydrocarbon residues present. The analysis made use of pentacyclic triterpanes as the long-term petroleum biomarkers for two known major oil spills.

Grahl-Nielsen *et al.* [38] used a method based on separation of the aliphatic fraction of oil followed by GC-MS detection of polycyclic alkanes for identification of two oil slicks off Norway. Of the polycyclic aliphatics used as biomarkers, the pentacyclic triterpanes were found to be better for the identification than steranes. The effect of weathering was also clearly demonstrated as virtually all components below nC13 had disappeared from one of the oils 9 days after the spill and components in the nC13-C17 region had been partly reduced. They also reported that as a result of weathering, the relative amount of components of low volatility increased with increasing complexity of composition. Wang and Fingas [28] have also used triterpanes and steranes as biomarkers in studies of the effects of weathering and concentration changes of crude oils. The authors used GC-MS to detect the relative abundance ratios of several pairs of triterpane and sterane compounds in eleven intertidal sediment samples containing weathered oil. The sediment samples were collected from Chedabucto Bay, Nova Scotia, which was the site of an oil spill in 1970 by the vessel *Arrow*. The authors were able to use triterpane/sterane ratios to determine that the *Arrow* was the source of the petroleum compounds. In addition, they found that the relative abundance ratios of several pairs of triterpane and sterane compounds, especially the ratio of C29/C30 hopanes, were independent of weathering effects and could unambiguously be used for identifying oil sources.

Now that many methods have been successfully developed and used for analyzing and monitoring weathering in crude oils, what more can be done? At present, enough is known to perform some type of separation and analysis of a crude oil fraction in order to study its degradation. However, the main method presently in use is one that was initially developed about

sixteen years ago. One would think that with advances in technology and continuing research in the environmental field, a new method would have evolved offering a means for validation or substantiation of old methods. Collaboration between environmental chemists and toxicologists who are presently working in this field could contribute substantially to this area. Future research involving electrospray ionization mass spectrometry may provide new insight into the analysis of crude oil fractions. Perhaps this method could also be applied to weathering studies to help scientists better understand how crude oil weathers in the environment. With more information, remediation experts may be able to develop technologies that will minimize the impact of the next big oil spill.

1.2 References

1. Fingas, M.F., Duval, W.S., and Stevenson, G.B. The basics of oil spill cleanup. Minister of Supply and Services Canada **1978**.
2. Moriarity, F. The study of pollutants in ecosystems, 3rd edition (Academic Press, London, UK and San Diego, CA, **1999**) pp. 275-278.
3. Rudzinski, W.E., and Aminabhavi, T.M. A review on extraction and identification of crude oil and related products using supercritical fluid technology. *Energy & Fuels* 14 (**2000**) 464-475.
4. Philp, R.P. and F.X. de las Heras. Fundamentals and applications of chromatography and related differential migration methods, *In* Chromatography, 5th edition, Journal of Chromatography Library – Volume 51B, *Edited by* E. Heftmann (Elsevier Applied Science Publishers, Amsterdam, **1992**) pp. B461-B473.
5. Black, J.A., Birge, W.J., Westerman, A.G., and Francis, P.C. Comparative aquatic toxicology of aromatic hydrocarbons. Fundam. Appl. Toxicol. 3:353-358 (**1983**).
6. Brunstrom, B., Broman, D. and Naf, C. Embryotoxicity of polycyclic aromatic hydrocarbons (PAHs) in three domestic avian species, and of PAHs and coplanar polychlorinated biphenyls (PCBs) in the common eider. *Environ. Pollut.*, 67 (**1990**) 133-143.
7. Germaine, A.F., Perron, F., and Van Coillie, R. PAHs in the environment: fate, ecotoxicity and regulations, Environment Canada, Conservation and protection, Quebec Region, Montreal, QC (**1993**).
8. Mansfield, C.T., Barman, B.N., Thomas, J.V., Mehrotra, A.K., McCann, J.M. *Anal. Chem.*

(**1999**), 71, 81R-107R.

9. Wang, Z. and Fingas, M., Developments in the analysis of petroleum hydrocarbons in oils, petroleum products and oil-spill-related environmental samples by gas chromatography, *J. Chromatogr. A,* 774 (**1997**) 51-78.
10. Ali, M.F., Bukhari, A., Hasan, M. *Fuel Sci. Technol. Int.* 7 (**1989**) 1179-1208.
11. Akhlaq, M.S. Rapid group-type analysis of crude oils using high-performance liquid chromatography and gas chromatography. *J. Chromatogr.*, 644 (**1993**) 253-258.
12. Ruckmick, S.C. and Hurtubise, R.J. Liquid chromatographic systems for the separation of polycyclic aromatic hydrocarbons and nitrogen heterocycle compounds present in coal liquids, *J. Chromatogr.,* 321 (**1985**) 343-353.
13. Frolov, E.B., Liquid chromatography of petroleum carbazoles, *Org. Geochem.* 26, No. ½, (**1997**) 43-47.
14. Schmitter, J-M., Colin, H., Excoffier, J-L., Arpino, P., and Gulochon, G. Identification of triaromatic nitrogen bases in crude oils, *Anal. Chem.* 54 (**1982**) 769-772.
15. Snyder, L.R. and Buell, B.E., Nitrogen and oxygen compound types in petroleum, *Anal. Chem.* 40 (**1968**) 1295-1302.
16. Snyder, L.R., Buell, B.E., and Howard, H.E., Nitrogen and oxygen compound types in petroleum: Total analysis of a 700-850 °F distillate from california crude oil. *Anal. Chem.* 40, No. 8 (**1968**) 1303-1317.
17. Mao, J., Pacheco, C.R., Traficante, D.D., Rosen, W. Analysis of neutral nitrogen compounds in diesel oil by direct injection high-performance liquid chromatography-mass spectrometry-ultaviolet spectrometry methods. *J. Chromatogr. A,* 684 (**1994**) 103-111.

18. Later, D.W., Lee, M.L., Bartle, K.D., Kong, R.C., and Vassilaros, D.L., Chemical class separation and characterization of organic compounds in synthetic fuels. *Anal. Chem.* 53 (**1981**) 1612-1620.

19. Schiller, J.E., and Mathiason, D.R. Separation method for coal-derived solids and heavy liquids. *Anal. Chem.* 49, No. 8 (**1977**) 1225-1228.

20. Ford C.D., Holmes, S.A., Thompson, L.F., and Latham, D.R. Separation of nitrogen compound types from hydrotreated shale oil products by adsorption chromatography on basic and neutral alumina. *Anal. Chem.* 53 (**1981**) 831-836.

21. Li, M., Larter, S.R., and Stoddart, D. Liquid chromatographic separation schemes for pyrrole and pyridine nitrogen aromatic heterocycle fractions from crude oils suitable for rapid characterization of geochemical samples. *Anal. Chem.* 64 (**1992**) 1337-1344.

22. Stefanova, M. and Lazarov, L., Gas chromatography-mass spectrometry study of coal-derived ssphaltenes, II. Carbazole-type neutral nitrogen compounds, *J. Chromatogr.*, 446 (**1988**) 293-304.

23. Wang, Z., Fingas, M., Li, K., Fractionation of a light crude oil and identification and quantification of aliphatic, aromatic, and biomarker compounds by GC-FID and GC-MS, Part I, *Journal of Chromatographic Science*, Vol. 32, (**1994**) 361-366.

24. Wang, Z., Fingas, M., Differentiation of the source of spilled oil and monitoring of the oil weathering process using gas chromatography-mass spectrometry, *J. Chromatogr. A,* 712 (**1995**) 321-343.

25. Wang, Z., Fingas, M., Landriault, M., Sigouin, L., Nanni, X., Identification of alkylbenzenes and direct determination of BTEX and (BTEX + C_3-Benzenes) in oils by GC/MS, *Anal.*

Chem., Vol. 67, No. 19 (**1995**) 3491-3500.

26. Wang, Z., Fingas, M., Landriault, M., Sigouin, L., Yuepeng, F., Mullin, J., Using systematic and comparative analytical data to identify the source of an unknown oil on contaminated birds, *J. Chromatogr. A,* 775 (**1997**) 251-265.
27. Wang, Z., Fingas, M., Sergy, G., Chemical characterization of crude oil residues from an arctic beach by GC/MS and GC/FID, *Environ. Sci. Technol.*, Vol. 29, No. 10 (**1995**) 2622-2631.
28. Wang, Z., Fingas, M., Sergy, G., Study of 22-year-old arrow oil samples using biomarker compounds by GC/MS, *Environ. Sci. Technol.*, Vol. 28, No. 9 (**1994**) 1733-1748.
29. Wang, Z. and Fingas, M., Study of the effects of weathering on the chemical composition of a light crude oil using GC/MS GC/FID, *J.Microcolumn Separations* 7 (6) (**1995**) 617-639.
30. Ignatiadis, I., Kuroki, M., and Arpino, P.J. Identification of carbazole derivatives in a hydrotreated coker gas oil by gas chromatography and gas chromatography-mass spectrometry. *J. Chromatogr.*, 366 (**1986**) 251-260.
31. Brumley, W.C., Brownberg, C.M., and Brilis, G.M. Characterization of nitrogen-containing aromatic compounds in soil and sediment by capillary gas-chromatrography-mass spectrometry after fractionation. *J. Chromatogr.,* 558 (**1991**) 223-233.
32. Guan, S., and Marshall, A.G. Resolution and chemical formula identification of aromatic hydrocarbons and aromatic compounds containing sulfur, nitrogen, or oxygen in petroleum distillates and refinery streams. *Anal. Chem.*, 68 (**1996**) 46-71.
33. Zhan, D., and Fenn, J.B. Electrospray mass spectrometry of fossil fuels. *Int J Mass Spectrom*, 194 (**2000**) 197-208.

34. Willard, H.H., Merritt, L.L.Jr, Dean, J.A., Settle, F.A. Jr. Instrumental methods of analysis. Wadsworth Publishing Company **1988**.

35. Fedorak, P.M., and Westlake, D.W.S. Microbial degradation of alkyl carbazoles in Norman Wells crude oil. *Appl. Environ. Microbiol.* Vol. 47, No. 4 (**1984**) 858-862.

36. Dutta, T.K. and Harayama, S. Analysis of long-side-chain alkylaromatics in crude oil for evaluation of their fate in the environment. *Environ. Sci. Technol.* 35 (**2001**) 102-107.

37. Page, D.S., Foster, J.C., Fickett, P.M., and Gilfillan, E.S. Identification of petroleum sources in an area impacted by the *Amoco Cadiz* oil spill. *Mar. Pollut. Bull.* Vol. 19, No. 3 (**1988**) 107-115.

38. Grahl-Nielsen, O. and Lygre, T. Identification of samples of oil related to two spills. *Mar. Pollut. Bull.* Vol. 21, No. 4 (**1990**) 176-183.

Chapter 2 - Techniques

2.1 Electrospray Ionization Mass Spectrometry (ESI-MS)

Electrospray-Ionization is a process that enables ions in solution to be analyzed easily in a mass spectrometer. The sample solution is introduced into a capillary at a flow rate usually between 1 and 50 μl/min. A high potential is applied to the capillary causing the solution to become charged as it exits through a needle tip. The solution emerges as a mist of highly charged droplets which pass down a potential and pressure gradient towards the analyzer portion of the mass spectrometer [1]. This is achieved using the flow of a bath gas which also assists with the evaporation of solvent from the charged droplets. The solvent evaporation leads to size reduction of the droplet and an increased surface tension. As the charge density on each droplet increases, a Coulomb explosion occurs which tears the droplet apart and produces smaller offspring droplets. The process continues until fully desorbed solute ions remain. Solute species that are not ionic can attach solute cations or anions to their polar groups and desorb from the droplet as so-called quasimolecular ions suitable for mass analysis [2]. Sampling of fully or partially desolvated ions is made using a capillary or skimmer (counter-electrode) device as illustrated in Figure 1.

In ESI-MS, a sample is ionized using the electrospray process and the resulting ions are collected in a mass analyzer. The analyzer separates the ions according to their different mass to charge ratios. The mass spectrometer in our laboratory is equipped with a quadrupole mass analyzer and generates a quadrupole field from four electrically conducting parallel rods. The

quadrupole is configured with opposite pairs of electrodes electrically connected; one pair of rods is held at positive direct current (+d.c.) and the other at –d.c.

Ions generated from the electrospray process are directed into the quadrupole where they travel down a longitudinal z-axis and undergo transverse motion in the x- and y-planes perpendicular to the longtitudinal axis [3]. The radio frequency (r.f.) field that is generated causes positive ions to be focused in the positive field and negative ions in the negative field. The ions oscillate down the quadrupole with increasing amplitude until they eventually collide with one of the electrodes. However, the d.c. and r.f. amplitudes on a mass spectrometer can be adjusted so that ions of all masses can sequentially pass through the quadrupole and be collected by the detector. In this way, a mass spectrum of all ions in the sample can be obtained.

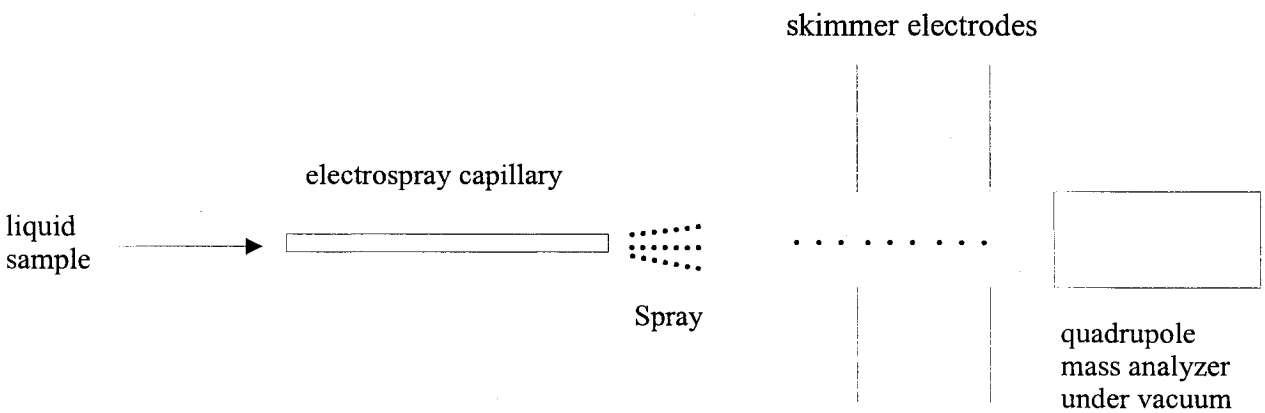

Figure 1. General features of an electrospray interface.

2.2 Electrospray Ionization Tandem Mass Spectrometry (ESI-MS/MS)

A common configuration for quadrupole mass spectrometers is the triple-quadrupole array enabling the instrument to perform tandem mass spectrometry. This setup consists of three quadrupoles in a linear configuration. The first and last quadrupoles are operated with d.c. and r.f. voltages allowing them to function as mass filters, while the middle quadrupole functions in r.f. mode only. Ions from the electrospray enter the first quadrupole where only those of a selected mass/charge (m/z) ratio are allowed to pass through to the second (middle) quadrupole. A collision gas is introduced into the middle chamber causing low energy collision-induced dissociation (CID) of the selected ions. To increase the internal energy of the selected ions from the first quadrupole, a collision energy (0-200 eV) may be applied to the ions before they enter the middle chamber. Finally, the fragment ions pass to the third quadrupole where they are mass filtered for detection. The resulting CID mass spectrum contains peaks for all fragment ions that were detected during the experiment, an achievement made possible by the focusing property of the second quadrupole. A positive ion traveling towards the negative rod of the quadrupole will undergo a change in direction due to a polarity switch from negative to positive on the rod. The result is that all fragment ions inside the middle quadrupole stay focused toward the center of the chamber, enabling them to pass through to the last quadrupole.

2.3 Experimental Procedures

All mass spectra were obtained using a Micromass Quattro-LC© triple-quadrupole mass spectrometer fitted with a Z-Spray© ion source and running the MassLynx© data acquisition and processing software. Typically, 5-10 µl of a sample was injected into a mobile phase of the same solvent composition at a flow rate of 20-50 µl/min. The inlet capillary voltage was held between + 4.0 and 4.5 keV (positive ion mode), and cone and extractor voltages adjusted as needed to obtain a stable signal. The nitrogen desolvation gas flow rate was 100 L/h. ESI-MS spectra were obtained over various *m/z* ranges.

Collision-induced dissociation mass spectra were recorded using the triple-quadrupole operating in MS/MS mode with argon collision gas in the rf-only hexapole. The CID mass spectrum of a compound will depend on the employed experimental conditions. For these experiments, cone, entrance, and exit voltages were optimized to produce the best spectra. A constant collision gas pressure of ~2.5 ± 0.5 x 10^{-4} mbar was used for all experiments reported here. Collision energy (laboratory frame) has a much more dramatic impact on the CID mass spectra. For the initial experiments, collision energy was varied to determine the best setting for fragmentation. For the CID experiments, collision energies in the range 20-100 eV were used and are indicated in the text. For all experiments, the analyzer (back) quadrupole low and high molecular mass resolutions were set between 12 and 15.

2.4 References

1. Gaskell, S. Electrospray: Principles and Practice. *J. Mass Spectrom.* 32, 677-688, **1997**.
2. Fenn, J. B.; Mann, Matthias; Meng, K.M.; Wong, S. F.; Whitehouse, C. M. Electrospray ionization-principles and practice. *Mass Spec. Revs.* 9, 37-70, **1990**.
3. Willard, H. H.; Merritt, L. L. Jr.; Dean, J. A.; Settle, F. A. Jr. Instrumental methods of analysis; 7th Ed., Wadsworth Publishing Company: California, **1988**.

Chapter 3 - Differentiation of Pyridine, Indole, Quinoline, and Carbazole Compounds using Electrospray-Ionization Tandem Mass Spectrometry

3.1 Introduction

The differentiation of isomeric compounds, apart from being an interesting academic pursuit, has wide spread applications in chemistry and biology. It is well known that often only certain isomeric forms of a compound are biologically active [1-3]. This has applications in the study of the environment as different isomers may biodegrade at different rates [4-7]. One example is the analysis of polychlorinated biphenyl contamination where it is known that some congeners biodegrade faster than others [7]. This opens up the possibility of determining the age of an environmental contaminant by identifying and quantifying the individual isomers of a particular compound [8,9].

Nitrogen-containing aromatic compounds (NCACs) such as substituted pyridines, indoles, quinolines and carbazoles are known to occur in the low to high molecular weight fractions of crude oil. However, the complex nature of these oils preclude easy identification of heterocycles without some form of preliminary fractionation. Hence, there are many reports on chemical class separation schemes for polar NCACs in oils, most of which employ solvent partitioning methods and column chromatography [10-15]. Some of these schemes when combined with gas chromatography or mass spectrometry have been useful in the identification of isomers [10-11]. In the literature, there are several reports on the use of mass spectrometric

applications for the differentiation of isomeric NCACs [16-20]. Vairamani *et al.* [16] revealed distinguishable spectra for alkyl, amino, hydroxy, cyano, and halo isomers of substituted pyridines using acetone chemical ionization mass spectrometry (CI-MS). Experiments on protonated pyridines, quinolines, and other related compounds have also been performed by Maquestiau *et al.* [18] using mass analyzed ion kinetic energy spectrometry (MIKE), and Daishima *et al.* [19] using collision induced dissociation (CID) chemical ionization mass spectrometry. Differences among isomers were more evident in the data of the former than that of the latter.

The objective of this research was to use ESI-MS/MS alone to distinguish between chemicals of different classes. The collision-induced dissociation mass spectra of a variety of pyridines, indoles, quinolines, and carbazoles were obtained and compared in order to differentiate the individual compounds.

3.2 Materials and Methods

The CID mass spectrum of a compound will depend on the employed experimental conditions. To this end, an assessment was made of the effect of collision gas pressure on the appearance of the CID mass spectra of protonated 3-methylpyridine. Varying the collision gas pressure affected the total fragment peak abundance but did not significantly affect the overall dissociation characteristics of protonated 3-methylpyridine (Table 1). Therefore, a collision gas

pressure of 2.5 ± 0.5 x 10^{-4} mbar was used for all experiments reported here.

Table 1. Effect of collision gas pressure on the CID mass spectrum of protonated 3-methylpyridine (*m/z* 94) at 25 eV.

m/z	Relative peak intensities				
	Collision gas pressure (10^{-4} mbar)				
	1.5	2.5	3.5	4.5	5.5
79	100	100	100	100	100
78	66	58	55	59	62
77	8	7	6	8	7
68	2	1	1	1	1
67	53	51	42	44	41
65	31	24	25	37	36
54	2	1	1	1	1
53	53	65	56	61	59
52	12	12	11	16	19
51	10	12	11	15	15
42	8	11	12	7	5
41	97	95	84	90	66
39	8	6	5	4	4
28	5	2	2	2	2
27	2	4	4	2	3

An assessment was also made of the effect of cone voltage on the appearance of the CID mass spectra of protonated 3-methylpyridine. Similar to the gas pressure studies, varying the cone voltage did not significantly affect the overall dissociation characteristics of protonated 3-methylpyridine (Table 2). The effect of collision energy on CID spectra was investigated for all three methylpyridines. Collision energy (laboratory frame) had a much more dramatic impact on the CID mass spectra, as expected. Figure 2 shows the energy dependence of several of the peaks in the CID mass spectra for the protonated methylpyridines as a function of laboratory

collision energy. The trends for each fragment ion were found to be consistent between measurements made during different experiments. The significance of the results will be discussed in more detail in the Results section, but for the purposes of the experimental procedures described herein, the results indicated that strict control of the collision energy was necessary to obtain reproducible results. A collision energy of 25 eV was used in all experiments discussed in this chapter, unless stated otherwise.

Table 2. Effect of cone voltage on the CID mass spectrum of protonated 3-methylpyridine (*m/z* 94) at 25 eV.

m/z	Relative peak intensities Cone Voltage (V)				
	20	40	60	80	100
79	100	100	100	100	81
78	58	58	56	69	50
77	7	7	8	6	10
68	1	1	1	2	2
67	48	51	51	41	68
65	28	24	26	28	31
54	1	1	2	2	2
53	53	65	75	79	92
52	12	12	14	12	20
51	8	12	9	7	15
42	8	11	10	10	12
41	91	95	81	88	100
39	4	6	5	5	6
28	2	2	3	2	2
27	2	4	5	7	4

(a)

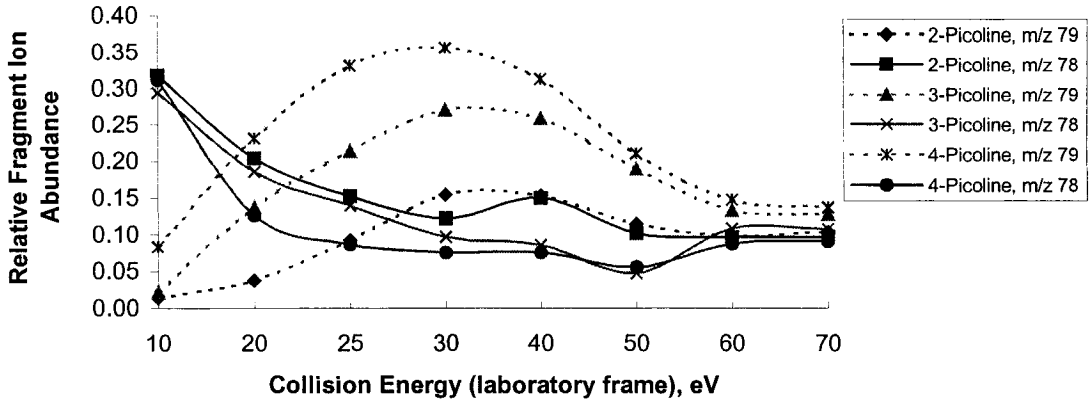

(b)

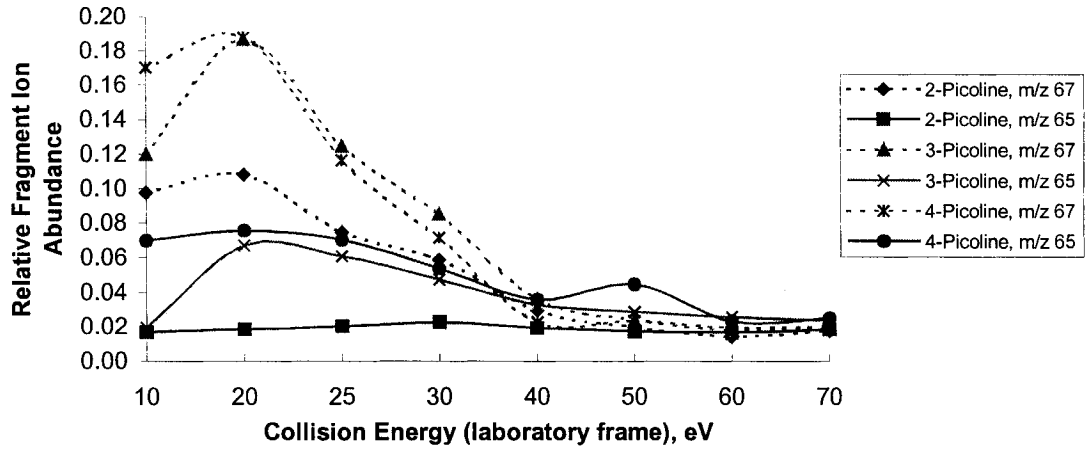

(c)

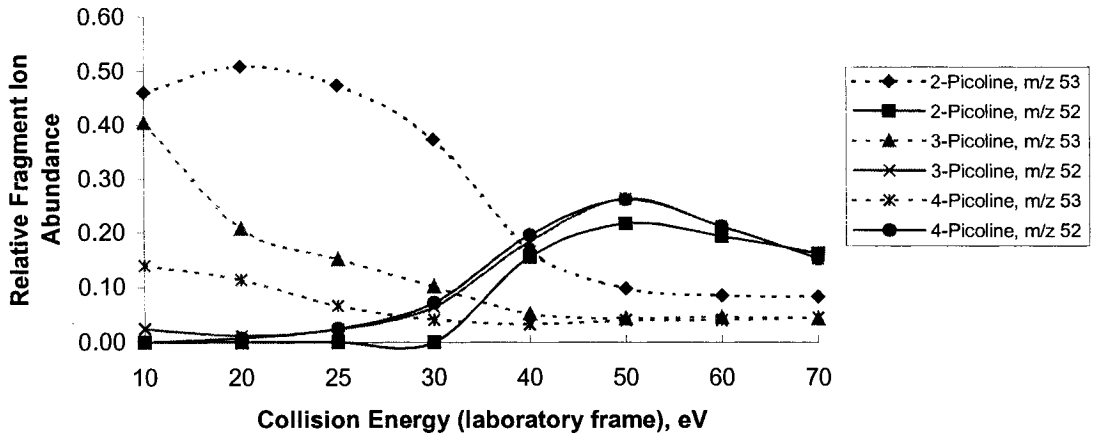

Figure 2. Energy dependence of fragment peaks of methylpyridines (Picolines) as a function of collision energy.

Samples of heterocyclic compounds were made available to our laboratory by the Emergencies Science Division of Environment Canada in Ottawa. These compounds had been purchased from Aldrich (95-99% purity) and prepared in benzene (10 000 ppm). Subsamples suitable for analysis by ESI were prepared in acetonitrile (~ 100 ppm). Typically, 5-10 μl of sample was injected into a 50% acetonitrile/water mobile phase having a flow rate of 20 μl/min.

Due to the instability of these compounds in air, GC-MS was conducted on the stock samples and all compounds were found to be pure. The chemicals studied are listed in Table 3. Perdeuterated 2-methylpyridine and 2,3-dimethylpyridine (99% purity, 99.5% isotopic enrichment) were obtained from C/D/N Isotopes Inc. (Point-Claire, QC) and prepared at 100 ppm in HPLC grade acetonitrile; 4-methylpyridine was obtained from Aldrich (99% purity).

Table 3. Heterocycles used in Electospray Experiments.

Chemical	**Structure**
2-Methylpyridine	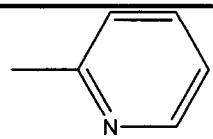
2-Methylpyridine d_7	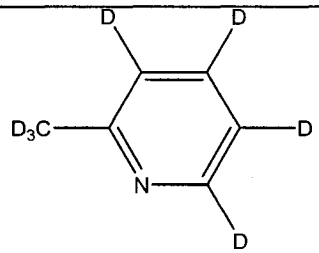
3-Methylpyridine	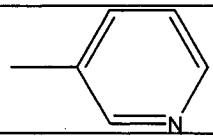

4-Methylpyridine	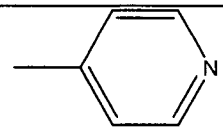
2-Ethylpyridine	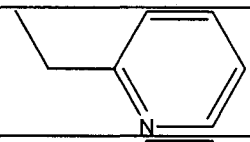
4-Ethylpyridine	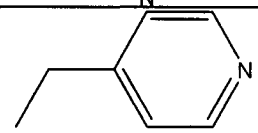
3-n-Butylpyridine	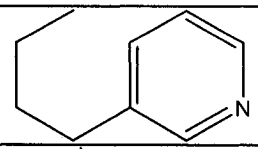
4-t-Butylpyridine	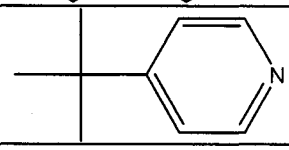
2,3-Dimethylpyridine	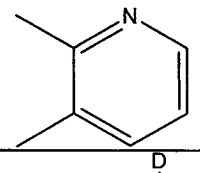
2,3-Dimethylpyridine d_9	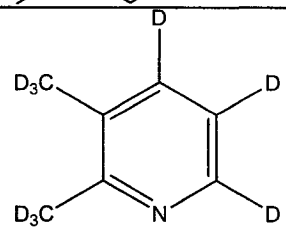
2,4-Dimethylpyridine	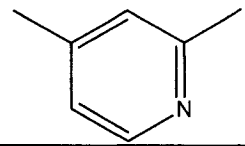
2,6-Dimethylpyridine	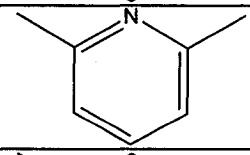
3,4-Dimethylpyridine	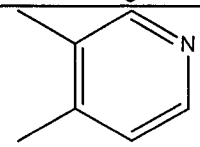

2,4,6-Trimethylpyridine	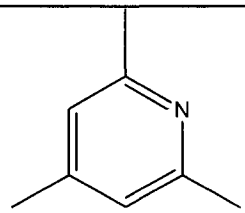
3-Hydroxypyridine	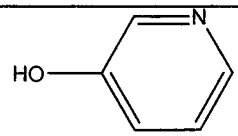
3-Hydroxy-2-methylpyridine	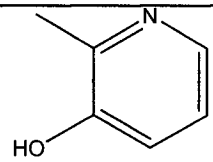
2-Hydroxy-4-methylpyridine	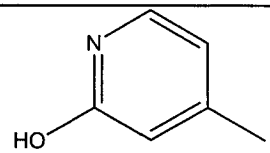
2-Phenylpyridine	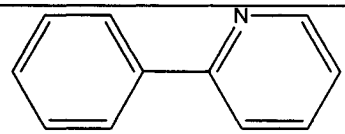
4-Phenylpyridine	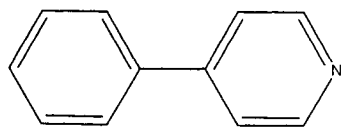
1-Methylindole	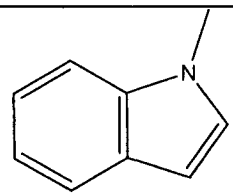
2-Methylindole	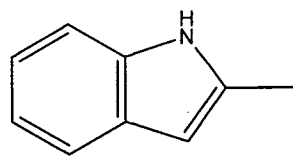

3-Methylindole	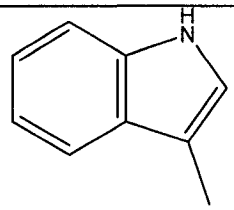
5-Methylindole	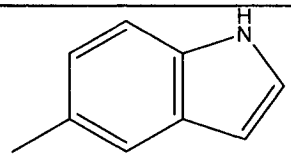
7-Methylindole	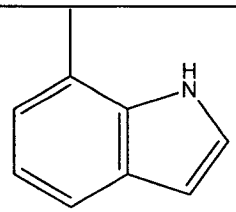
1,2-Dimethylindole	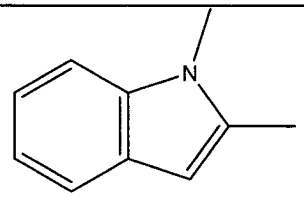
2,3-Dimethylindole	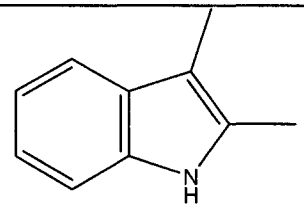
3-Methylquinoline	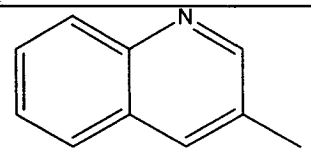
4-Methylquinoline	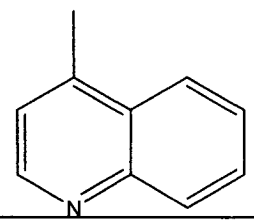

8-Methylquinoline	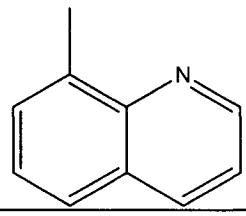
2,4-Dimethylquinoline	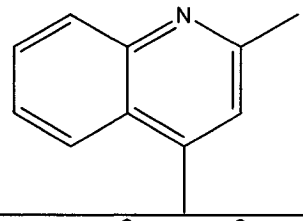
2,7-Dimethylquinoline	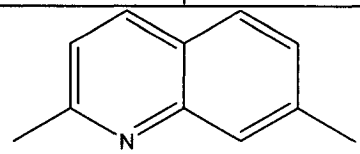
2-Phenylquinoline	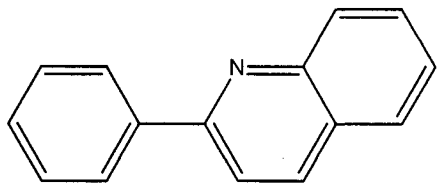
2-Methyl-8-hydroxyquinoline	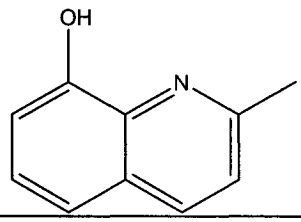
3-Hydroxyquinoline	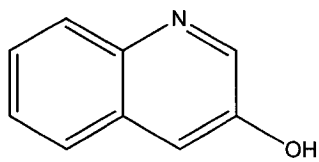
2,3-Benzoquinoline	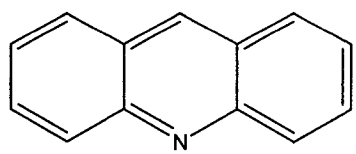

3,4-Benzoquinoline	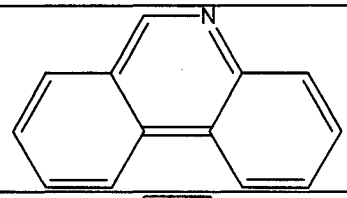
7,8-Benzoquinoline	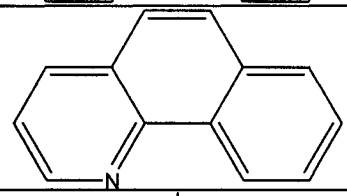
9-Methylcarbazole	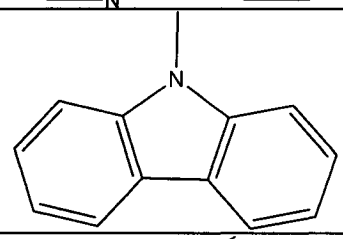
9-Ethylcarbazole	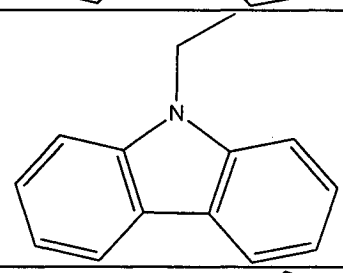
9-Phenylcarbazole	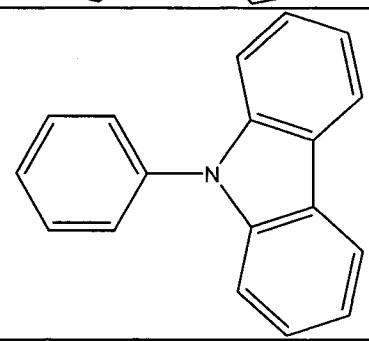
1,2,3,4-Tetrahydrocarbazole	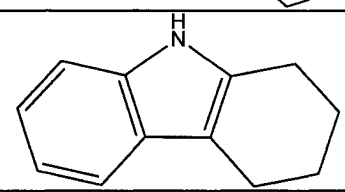
1,4,5,8,9-Pentamethylcarbazole	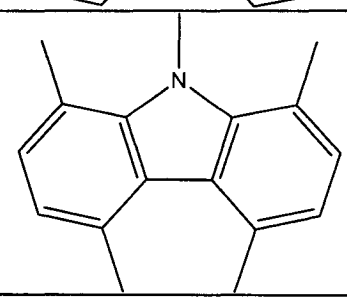

3.3 Results and Discussion

3.3.1 Pyridine Derivatives: Methyl Pyridines

The CID mass spectra (25 eV laboratory frame collision energy) of protonated 2-, 3- and 4-methylpyridine (*m/z* 94) are summarized in Figure 3. The three ions yield distinct mass spectra, distinguishable in the ratios of *m/z* 78 and 79, and *m/z* 53 and 41. The position of the methyl group has an observable influence on these fragment ion abundances. For *m/z* 79, corresponding to loss of 15 amu, the fragmentation is equally favorable for the 3- and 4- isomers, and much less so for the 2- isomer. A similar occurrence is observed in the relative abundances of *m/z* 41 and *m/z* 78 (see Table 4). However, for these peaks fragmentation is strongly favored for the 3-methyl isomer, less so for the 4-isomer, and even less for the 2-isomer. Loss of 41 amu (*m/z* 53) occurs more favorably for the 2-methyl isomer, followed by the 3- and then the 4-methyl isomer.

The CID mass spectrum of protonated 2-methyl pyridine-d_7 (*m/z* 101, Figure 4) aids in the identification of the fragment ions formed by the methyl pyridines. From 2-methyl pyridine d_7, *m/z* 83, 82 and 81 correspond to loss of CD_3, CD_3H and CD_4, respectively, indicating that for the methylpyridines, *m/z* 78 and 79 correspond to CH_4 and CH_3 loss. The intensity difference between *m/z* 81 and 82 indicates a 2 : 1 competition between the loss of the N-H and C-H for methane loss. The loss of CD_2H_2 (also *m/z* 83) cannot be discounted, but the absence of *m/z* 84

(CDH_3) indicates that the former channel is unlikely to be significant as there appears to be no loss of positional identity of the methyl hydrogens.

Table 4. Relative peak intensities in the CID mass spectra of protonated methylpyridines at 25 eV.

m/z	Relative peak intensities			Possible fragment ion
	2-methylpyridine	3-methylpyridine	4-methylpyridine	
79 $[MH-15]^+$	27	100	100	$C_5H_5N^+$
78 $[MH-16]^+$	42	58	30	$C_5H_4N^+$
77 $[MH-17]^+$	4	7	10	$C_5H_3N^+$
68 $[MH-26]^+$	1	2	4	$C_5H_8^+$
67 $[MH-27]^+$	19	51	27	$C_5H_7^+$
65 $[MH-29]^+$	5	24	16	$C_5H_5^+$
54 $[MH-30]^+$	1	1	3	$C_4H_6^+$
53 $[MH-41]^+$	100	65	16	$C_4H_5^+$
52 $[MH-42]^+$	7	12	8	$C_4H_4^+$ or $C_3H_2N^+$
51 $[MH-43]^+$	5	12	5	$C_4H_3^+$
42 $[MH-52]^+$	7	11	3	CH_3CNH^+
41 $[MH-53]^+$	16	95	52	$C_3H_5^+$
39 $[MH-55]^+$	1	6	4	$C_3H_3^+$
28 $[MH-66]^+$	1	2	5	CH_2N^+ or $C_2H_4^+$
27 $[MH-67]^+$	7	4	1	$C_2H_3^+$

These assignments are also consistent with the change in fragment ion intensity with increasing collision energy (Figure 2). The fragmentation channel responsible for *m/z* 78 is a low energy channel (since it is a dominant process at low collision energies), but the relative intensity of the channel decreases as the collision energy is raised, both observations indicating that the process likely occurs via a tight transitions state (entropy of activation, $\Delta S^{\ddagger}$, less than zero) and hence a rearrangement process (as would be expected for CH_4 loss) [25].

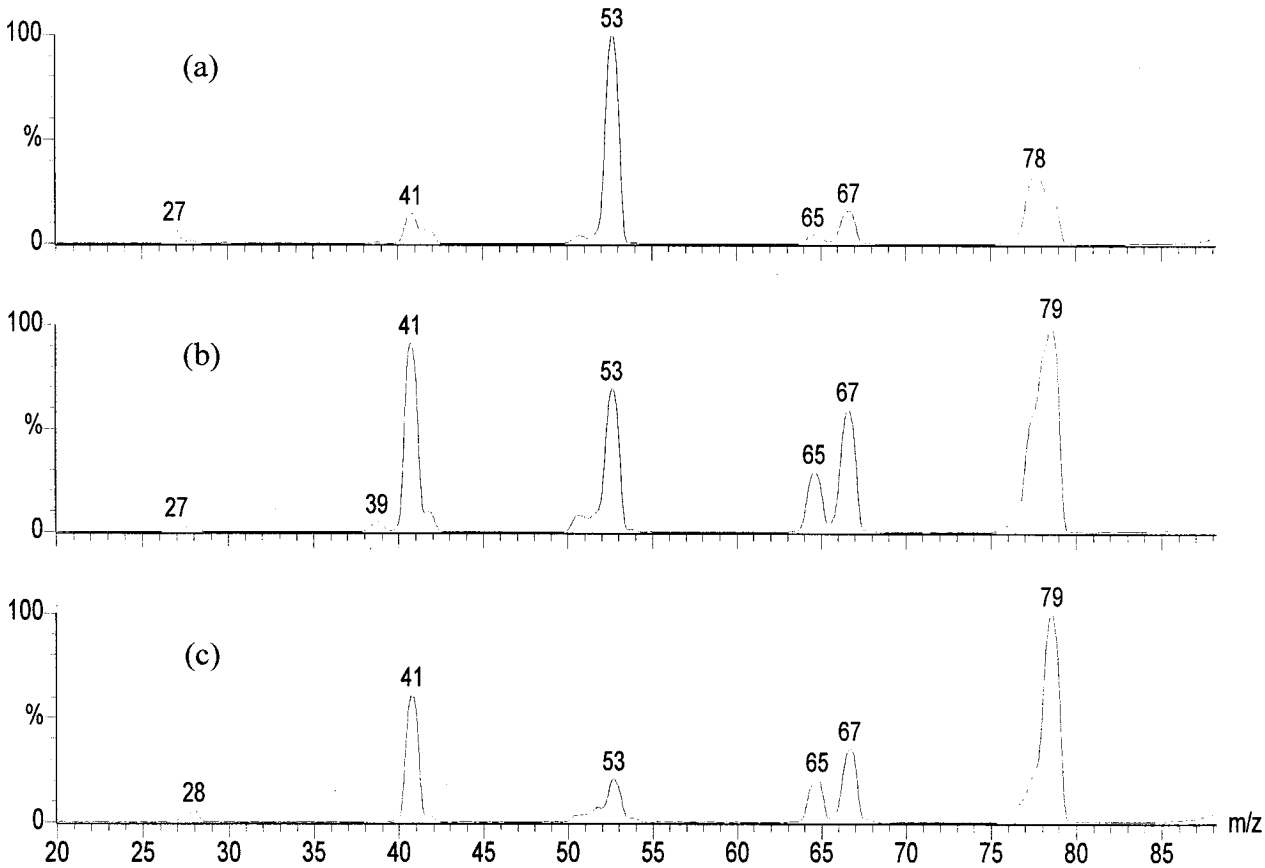

Figure 3. CID mass spectra of 2-methypyridine (a), 3-methylpyridine (b), and 4-methylpyridine (c) at 25 eV. Ordinate scale has been expanded.

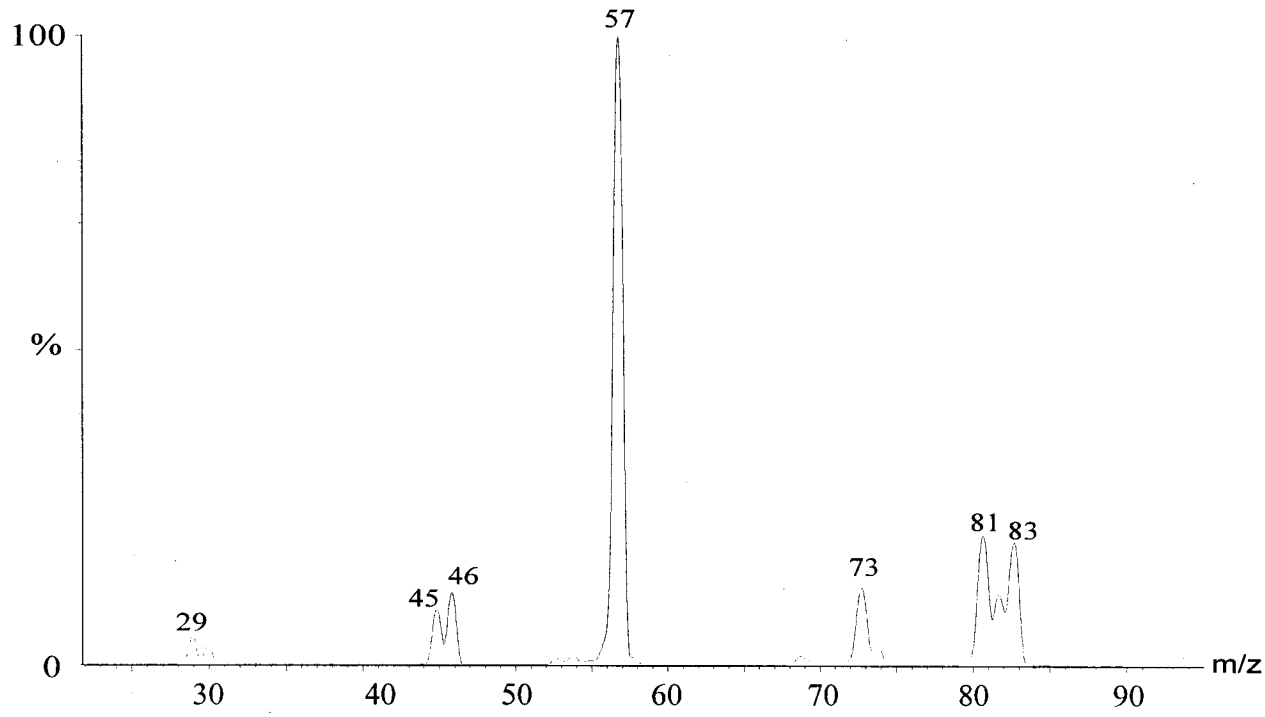

Figure 4. CID mass spectrum of 2-Methylpyridine d_7 at 25 eV. Ordinate Scale has been expanded.

Methyl loss (*m/z* 79) results from a simple bond dissociation and thus should occur via a loose transition state ($\Delta S^{\ddagger} > 0$) resulting in an increase in intensity with increasing collision energy. Competition from other processes results in a plateauing and subsequent drop in the *m/z* 79 signal (Figure 2).

The next prominent peak cluster is *m/z* 67 and 65 (Table 4). The former signal (loss of 27) was confirmed to be due to HCN loss, as the perdeuterated sample exhibits loss of 28 (DCN), *m/z* 73. The ion at *m/z* 67 is assumed to be $C_5H_7^+$, a fragment which has appeared in the spectra of other pyridine derivatives [17]. The ion at *m/z* 65 can only be due to the loss of CH_2NH, since loss of an ethyl group would result in a peak with *m/z* 67 in the perdeuterated ion, which is clearly absent in Figure 2. The peak at *m/z* 53 is shifted to *m/z* 57 in the d_7 spectra, indicating the incorporation of three deuterium atoms, and confirming this ion to be due to the loss of C_2H_3N (either CH_3CN or CH_2=N=CH). The energy dependence of *m/z* 53 also suggests this ion results from a low energy rearrangement process (Figure 2). It is plausible that the position of the CH_3 group adjacent to the protonated nitrogen atom in 2-methylpyridine makes the loss of C_2H_3N more facile than it is for protonated 3-, and 4-methylpyridine. The fragment ion at *m/z* 52 can be either $C_4H_4^+$ or $C_3H_2N^+$ while that at *m/z* 51 can be either $C_4H_3^+$ or C_3HN^+. The results from the d_7-ion indicate that *m/z* 51 can only be $C_4H_3^+$ (as C_3HN^+ would be present as either *m/z* 51 or *m/z* 52 in the d_7 spectrum, which are absent), while *m/z* 52 could be either possibility. The energy dependence of *m/z* 52 (Figure 2) suggests this ion is formed via a loose transition state and has a significant energy threshold. Formation of $C_3H_2N^+$ requires two separate hydrogen-transfer

reactions (to lose C_3H_6) while formation of $C_4H_4^+$ can conceivably be generated by the breaking of two bonds without atom rearrangement. This latter process may be more likely to have a high activation energy but a loose transition state. The ion at *m/z* 42 in all three methylpyridine spectra can be attributed to either CH_3CNH^+ or $C_3H_6^+$. The former ion would result in a peak with *m/z* 45 or 46 ($C_2D_3HN^+$ or $C_2D_4N^+$) in the mass spectrum of the d_7 ion, while the latter would occur as *m/z* 47 or 48 ($C_3D_5H^+$ or $C_3D_6^+$) in the spectrum, which are clearly absent. In a similar manner, the ion with *m/z* 41 that occurs in the mass spectra was confirmed to be $C_3H_5^+$ due to the absence of *m/z* 44 ($C_2D_3N^+$) in the d_7 spectrum. However, this is not the same ion that has been suggested by other researchers during mass spectrometry studies. Van Thuijl *et al.*[23] have generated four distinct *m/z* 41 ions of the form $C_2H_3N^{+\cdot}$ from several nitrogen-containing compounds. As well, the same ion has been assigned to the fragment at *m/z* 41 when appearing in the spectra of non-decomposing $C_4H_5N^{+\cdot}$ ions from several pyridine derivatives [17]. The peak with *m/z* 27 was confirmed to be $C_2H_3^+$ and not HCN^+ due to the absence of *m/z* 28 in the d_7-spectrum.

The energy dependence of several fragment ion signals for protonated 2-, 3- and 4-methyl pyridine (or picolines) are compared in Figure 2. It is readily observed that the fragment ions at *m/z* 78 and 79 for 3- and 4-methylpyridine respond similarly over the collision energy range 10-70 eV, with the *m/z* 79 channel being more favorable. For the 2- isomer, these two channels are very similar and equally favored. A similar effect is observed for fragment ions at *m/z* 65 and 67, but in this case all relative abundances tend to decrease to between 10-20% at 40 eV and remain at that level up to 70 eV. The last illustration clearly indicates that the fragment ion at *m/z* 53 is

more favored by the 2- isomer, followed by the 3- and then the 4- isomer. For *m/z* 52, this is an unfavorable fragmentation pathway for all isomers until a collision energy of 40 eV is reached.

3.3.2 Pyridine Derivatives: Dimethyl Pyridines

The CID mass spectra for the four isomeric protonated dimethylpyridines (*m/z* 108) are presented in Figure 5 (and Table 5). The differences between the isomers reside primarily in the relative peak intensities in these spectra. Loss of methyl (*m/z* 93) and methane (*m/z* 92) are competitive processes in each isomer, the former being favored strongly by protonated 2,4-dimethylpyridine. The proximity of a methyl substituent to the proton on nitrogen does not consistently favor methane loss. The results for protonated 2,3-dimethylpyridine-d_9 (Figure 6) indicate a 2:1 preference for the loss of methane (*m/z* 97 and 98) incorporating a hydrogen other than the one located on the nitrogen. This is consistent with the fact that methane elimination is not governed by the proximity of a methyl group to the proton on N. The collision energy dependence of methane loss from protonated 2,3- and 2,4-dimethylpyridine is qualitatively different from those for the other two isomers (Figure 7).

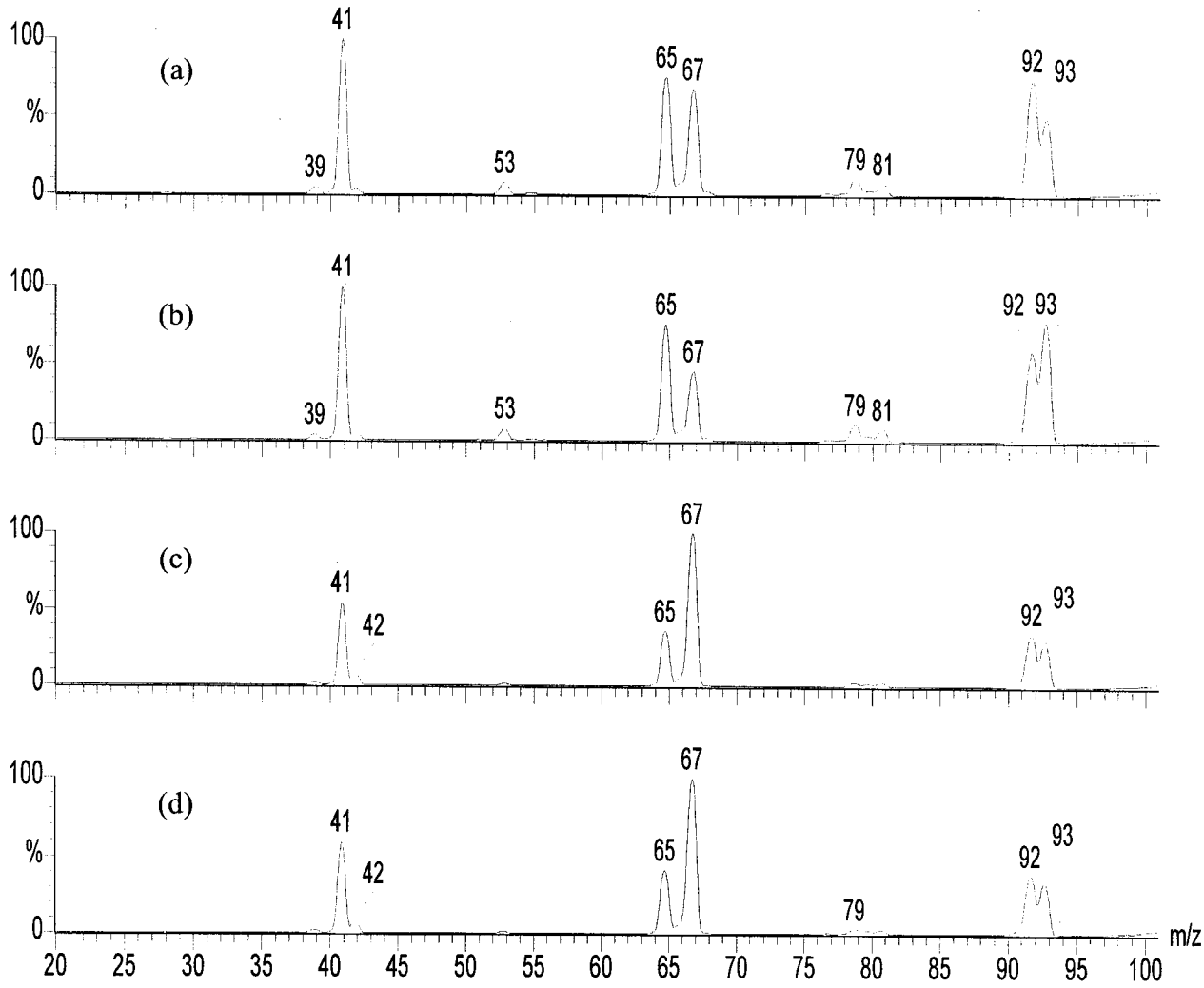

Figure 5. CID mass spectra of 2,3-dimethypyridine (a), 2,4-dimethylpyridine (b), 2,6-dimethyl-pyridine (c), and 3,4-dimethylpyridine (d) at 25 eV. Ordinate scale has been expanded.

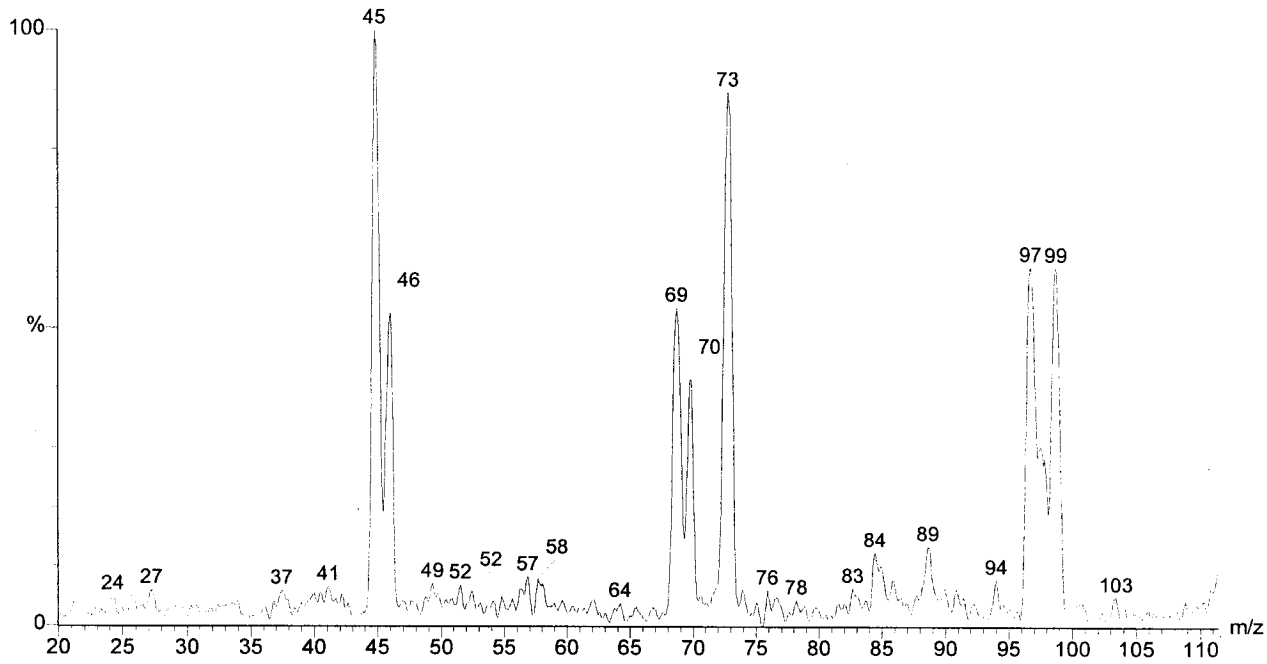

Figure 6. CID mass spectrum of 2,3 dimethylpyridine d_9 at 25 eV. Ordinate scale has been expanded.

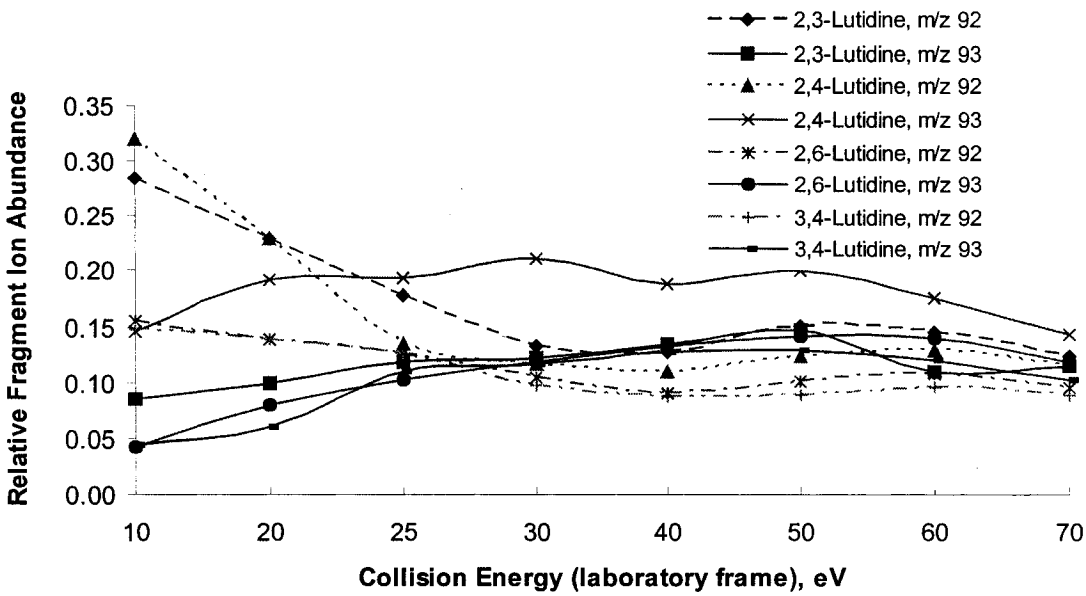

Figure 7. Energy dependence of methyl and methane loss from protonated dimethyl-pyridines (lutidines) as a function of collision energy.

Table 5. Relative peak intensities in the CID mass spectra of protonated dimethylpyridines at 25 eV.

m/z	Relative peak intensities			
	2,3-dimethyl	2,4-dimethyl	2,6-dimethyl	3,4-dimethyl
93 $[MH-15]^+$	50	79	28	33
92 $[MH-16]^+$	75	55	35	38
81 $[MH-27]^+$	7	7	3	2
80 $[MH-28]^+$	3	4	2	2
79 $[MH-29]^+$	10	10	2	3
77 $[MH-31]^+$	1	1	1	1
67 $[MH-41]^+$	68	45	100	100
66 $[MH-42]^+$	8	8	7	7
65 $[MH-43]^+$	76	74	36	42
53 $[MH-55]^+$	7	1	1	1
42 $[MH-66]^+$	3	6	7	8
41 $[MH-67]^+$	100	100	54	62

The other major fragmentation channels form *m/z* 67, 65 and 41. Isotopic labeling shows that these channels are analogous to those observed for the methylpyridines. The peak at *m/z* 67 corresponds to loss of C_2H_3N (loss of C_2D_3N in the labeled ion) while *m/z* 65 is formed by the loss of C_2H_5N (C_2D_5N and C_2HD_4N from the labeled ion). The ion at *m/z* 41 corresponds to $C_3H_5^+$ ($C_3HD_4^+$ and $C_3D_5^+$ in the labeled ion mass spectrum). A methyl group adjacent to the protonated nitrogen atom does not facilitate the loss of C_2H_3N as this channel is equally favorable for both 2,6- and 3,4-dimethylpyridine.

Methyl loss can be used to distinguish the 4-substituted isomers from the other two, and the two 4-substituted isomers are themselves distinguishable based on their ratios of *m/z* 93 : 41.

The isomers 2,3- and 2,6-dimethylpyridine are distinguished by their ratios of methyl to methane loss, the former ion favoring methane loss.

3.3.3 Pyridine Derivatives: Trimethyl Pyridine

Only one tri-methyl compound was studied, protonated 2,4,6-trimethyl pyridine (*m/z* 122). The CID mass spectrum is dominated by *m/z* 107 (the loss of CH_3), *m/z* 106 (loss of CH_4), *m/z* 79 (-43), *m/z* 53 (-69) and *m/z* 41. Assuming analogous behavior to the methyl and dimethyl isomers, *m/z* 79 can be assigned to the loss of C_3H_5N while *m/z* 41 is $C_3H_5^+$. Loss of 69 amu to form *m/z* 53 suggests this ion is formed by the loss of C_4H_7N since each of the methyl pyridines exhibit a related reaction in their mass spectrum. Protonated methyl pyridines were shown to lose C_2H_3N while the dimethyl ions lose C_3H_5N (see discussion presented above).

3.3.4 Pyridine Derivatives: Ethyl Pyridines

The CID mass spectra obtained for protonated 2- and 4-ethylpyridine (*m/z* 108) are shown in Figure 8. For both isomers, the dominant channel is methyl loss to form *m/z* 93, presumably generating the stabilized benzyl-type radicals protonated 2-pyridylmethyl or 4-pyridylmethyl. The distinction between the two isomers lies in the minor processes, notably in the losses of ethyl (*m/z* 79), ethane (*m/z* 78) and 41 amu (*m/z* 67) (see Table 6). Proximity to the pyridine nitrogen mitigates loss of ethyl in the 2-isomer and is due to the 2-pyridinium ion being stabilized by the lone pair on nitrogen [20].

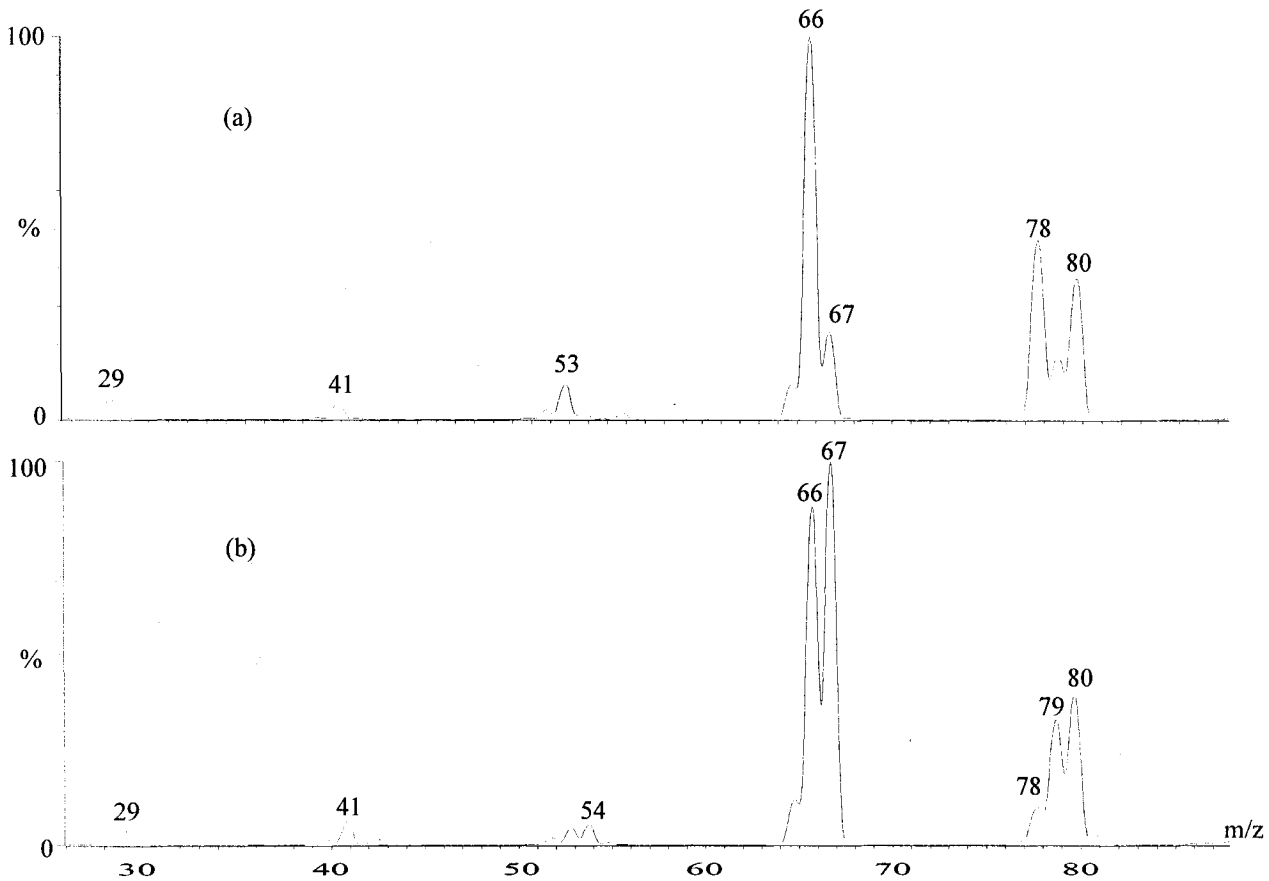

Figure 8. CID mass spectra of 2-ethylpyridine (a) and 4-ethylpyridine (b) at 25 eV from *m/z* 26 to *m/z* 88. Base peak is *m/z* 93 in both cases (Table 5). Ordinate scale has been expanded.

Table 6. Relative peak intensities in the CID mass spectra of protonated ethylpyridines at 25 eV for the m/z range 20-80.

m/z	Relative peak intensities	
	2-ethylpyridine	4-ethylpyridine
80 $[MH-28]^+$	37	40
79 $[MH-29]^+$	17	34
78 $[MH-30]^+$	47	10
67 $[MH-41]^+$	24	100
66 $[MH-42]^+$	100	88
65 $[MH-43]^+$	9	12
54 $[MH-54]^+$	2	6
53 $[MH-55]^+$	9	4
41 $[MH-67]^+$	4	6
29 $[MH-79]^+$	6	5

The preference of the 4-ethyl isomer for the loss of 41 amu suggests that this dissociation incorporates the side chain (C_3H_5 rather than C_2H_3N). In this, it is similar to the loss of 27 amu from the protonated methylpyridines, which is favored by the isomer with the side chain in the 3 position. The 2-ethyl isomer exhibits a strong loss of 42 amu (*m/z* 66) which can be due either to propene or C_2H_4N. Proximity to the proton on nitrogen enhances this channel thereby suggesting that the former process is the more likely.

3.3.5 Pyridine Derivatives: Butylpyridines

Protonated 3-*n*-butyl- and 4-*t*-butylpyridine (*m/z* 136) have isomeric side chains in addition to their different positions on the ring. The CID spectra of the ions are presented in Table 7. Dominant fragmentation pathways for the *t*-butyl isomer are methyl loss (*m/z* 121) and ethane loss (*m/z* 106), common channels for ions having the *t*-butyl group. The mass spectrum of the *n*-butyl isomer is dominated by the loss of a propyl group, likely forming the protonated 2-pyridylmethyl radical cation.

Table 7. Relative peak intensities in the CID mass spectra of protonated butylpyridines at 25eV.

m/z	Relative peak intensities	
	3-n-butylpyridine	4-t-butylpyridine
121 $[MH-15]^+$	-	75
120 $[MH-16]^+$	-	14
107 $[MH-29]^+$	2	-
106 $[MH-30]^+$	5	100
94 $[MH-42]^+$	6	-
93 $[MH-43]^+$	100	1
80 $[MH-56]^+$	1	3
79 $[MH-57]^+$	1	3
67 $[MH-69]^+$	1	-
66 $[MH-70]^+$	1	-
57 $[MH-79]^+$	1	1
41 $[MH-95]^+$	1	-

3.3.6 Pyridine Derivatives: Hydroxypyridines

The CID mass spectrum of 3-hydroxypyridine (*m/z* 96) is dominated by peaks at *m/z* 78 (water loss), *m/z* 68 (loss of CO) and *m/z* 41 ($C_3H_5^+$ from analogy to the methyl pyridines). Two isomers were also studied, protonated 2-hydroxy-4-methylpyridine and 3-hydroxy-2-methylpyridine (*m/z* 110); their CID mass spectra are presented in Figure 9. Since 2- and 4-hydroxypyridine exist as pyridones in aqueous solution [21, 22], the 2- isomer would be expected to do the same. However, it has been reported that 2-, 3-, and 4-hydroxypyridine exist in the enolic form in the gas phase [21]. For these two isomers then, it is difficult to speculate which form may predominate after ionization, as was concluded by Sakurai *et al.* [17] in their study of hydroxypyridines.

The most pronounced difference between the two isomers is their relative propensity for water loss. The 2-isomer exhibits a major peak for this loss, while it is only a minor process of the 3-isomer. As well, the relative peak intensity for water loss from 3-hydroxypyridine (31%) is almost three times that for 3-hydroxy-2-methylpyridine (11%) (see Table 8). Distinguishable differences in the CID mass spectra of 3- and 4-hydroxypyridine with that of 2-hydroxypyridine have previously been reported [16,17, 21]. As well, it has also been shown that loss of water occurs more favorably for methane adducts of 2-hydroxypyridine than for 4-hydroxypyridine (55% vs 11% peak abundances)[18]. This was attributed to the coexistence of both protonated amine and protonated hydroxy tautomers.

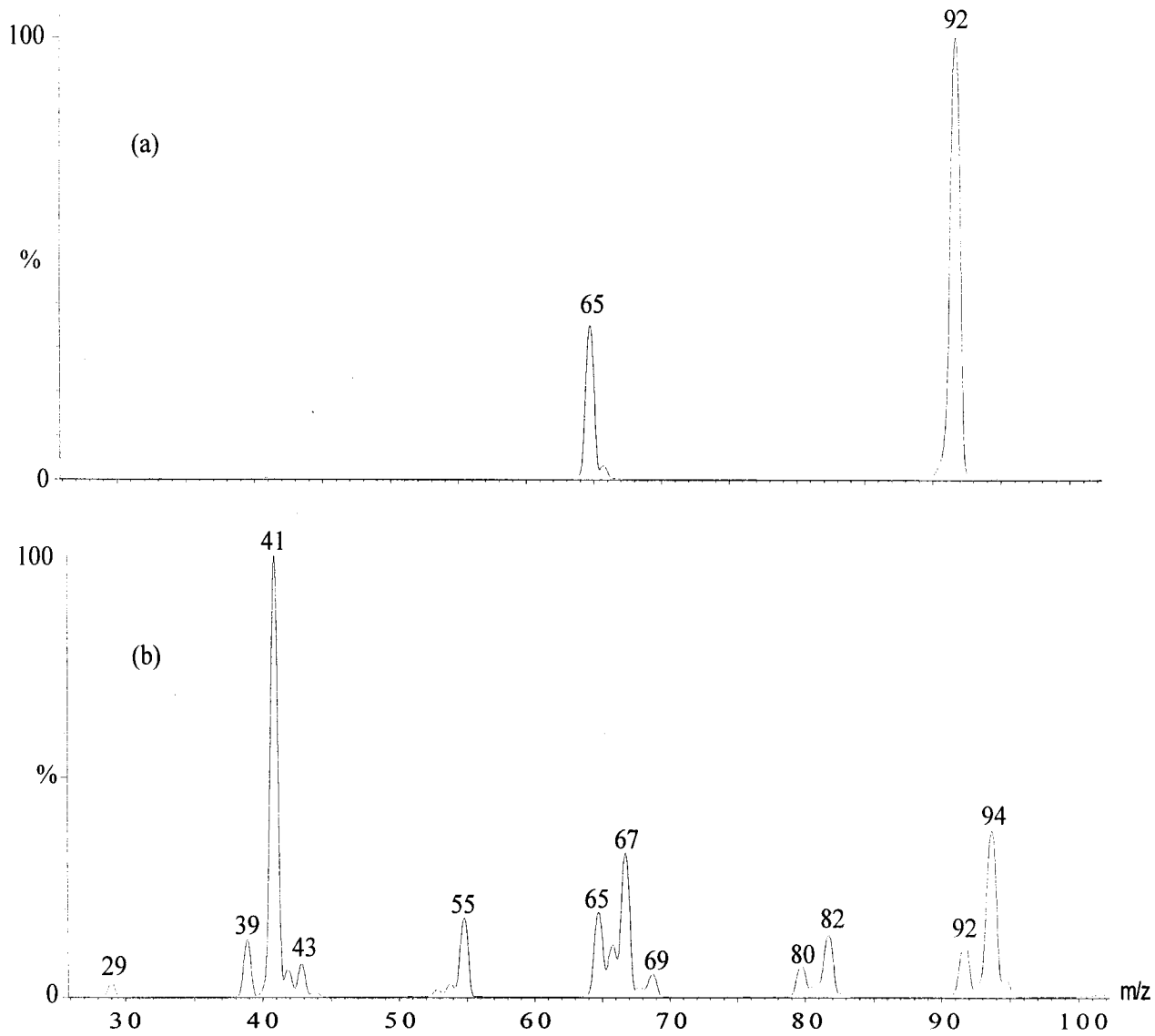

Figure 9. CID mass spectra of 2-hydroxy-4-methylpyridine (a) and 3-hydroxy-2-methylpyridine (b) at 25 eV. Ordinate scale has been expanded.

Table 8. Relative peak intensities in the CID (25 eV) mass spectra of protonated hydroxy-methylpyridines.

m/z	Relative peak intensities	
	3-hydroxy-2-methylpyridine	2-hydroxy-4-methylpyridine
95 $[MH-15]^+$	6	-
94 $[MH-16]^+$	36	-
93 $[MH-17]^+$	4	-
92 $[MH-18]^+$	11	100
82 $[MH-28]^+$	14	-
81 $[MH-29]^+$	5	-
80 $[MH-30]^+$	10	-
69 $[MH-41]^+$	5	-
68 $[MH-42]^+$	6	-
67 $[MH-45]^+$	42	-
66 $[MH-44]^+$	18	3
65 $[MH-45]^+$	26	35
55 $[MH-55]^+$	21	-
54 $[MH-56]^+$	6	-
43 $[MH-67]^+$	14	-
42 $[MH-68]^+$	9	-
41 $[MH-69]^+$	100	1
39 $[MH-71]^+$	24	1
29 $[MH-81]^+$	4	-

The results tend to agree with this theory and indicate that the hydroxy group of the 2-isomer is preferentially protonated in the gas phase as evidenced by strong loss of water in the CID spectrum. For 3-hydroxypyridine and 3-hydroxy-2-methylpyridine, it appears that both are preferentially protonated on the ring nitrogen as evidenced by much weaker peaks for water loss in the CID spectra.

3.3.7 Pyridine Derivatives: Phenylpyridines

The CID mass spectra of the protonated 2-phenylpyridine and 4-phenylpyridine (*m/z* 156) are summarized in Table 9. The channel producing *m/z* 78 can either form neutral benzene and a cation, $[pyridine\text{-}H]^+$, or the benzene radical cation and the $[pyridine\text{-}H]^{\bullet}$ radical. The former channel is the more likely as benzene is apt to have a larger ionization energy than the free radical $[pyridine\text{-}H]^{\bullet}$. Hydrogen transfer to the departing phenyl group is enhanced by its proximity to the proton on nitrogen. A significant distinguishing feature in the spectra is *m/z* 128 $[MH\text{-}28]^+$ and is due to loss of CH_2N^+.

Table 9. Relative peak intensities in the CID mass spectra of protonated phenylpyridines at 25 eV.

m/z	Relative peak intensities	
	2-phenylpyridine	4-phenylpyridine
141 $[MH\text{-}15]^+$	1	1
130 $[MH\text{-}26]^+$	1	3
129 $[MH\text{-}27]^+$	3	13
128 $[MH\text{-}28]^+$	7	83
127 $[MH\text{-}29]^+$	3	37
117 $[MH\text{-}39]^+$	1	3
104 $[MH\text{-}52]^+$	3	10
103 $[MH\text{-}53]^+$	1	4
80 $[MH\text{-}76]^+$	1	2
79 $[MH\text{-}77]^+$	-	3
78 $[MH\text{-}78]^+$	100	100
54 $[MH\text{-}102]^+$	1	22
53 $[MH\text{-}103]^+$	4	7
51 $[MH\text{-}104]^+$	2	3

Further CID studies were conducted on the ion at *m/z* 78 using in-source fragmentation followed by MS/MS. A cone voltage of 80 V and a collision energy of 25 eV were used. For the 4-phenyl isomer, the CID mass spectrum of *m/z* 78 produced fragment ions at *m/z* 52(3), 51(67), 50(8), 28(2), and 27(5). The 2-phenyl isomer gave a mass spectrum with fragment ions at *m/z* 52(8), 51(64), and 50(18). The slight differences may once again be due to the position of the phenyl group on the ring. It is proposed that the ion at *m/z* 78 fragments to i) HCN + $C_4H_3^+$ (*m/z* 51); ii) CH_2N + $C_4H_2^+$ (*m/z* 50); iii) C_2H_2 + the propiolonitrile ion $C_3H_2N^+$ (*m/z* 52).

3.3.8 Quinoline Derivatives: Methylquinolines

The CID mass spectra of protonated 3-methyl, 4-methyl and 8-methyl quinoline (*m/z* 144) are presented in Figure 10. The main distinguishing features are the peak intensities of *m/z* 77, *m/z* 103, *m/z* 115 and *m/z* 127 - 129 (see Table 10). The protonated methyl quinolines exhibit loss of methyl and methane (with the location of the methyl substituent on the pyridine ring increasing the relative probability of methane loss) and loss of ammonia. The position of the methyl group clearly determines the relative importance of the ammonia loss channel as it is a minor process in the fragmentation of protonated 8-methylquinoline, but is significant in the chemistry of the other two ions. Ammonia loss is expected to involve significant rearrangement of the quinoline ions, which is born out by the collision energy dependence of this channel (*m/z* 127) which is clearly that of a process occurring via a tight transition state (Figure 11a). Loss of 29 amu (*m/z* 115) can be either in the form of C_2H_5 or CH_3N.

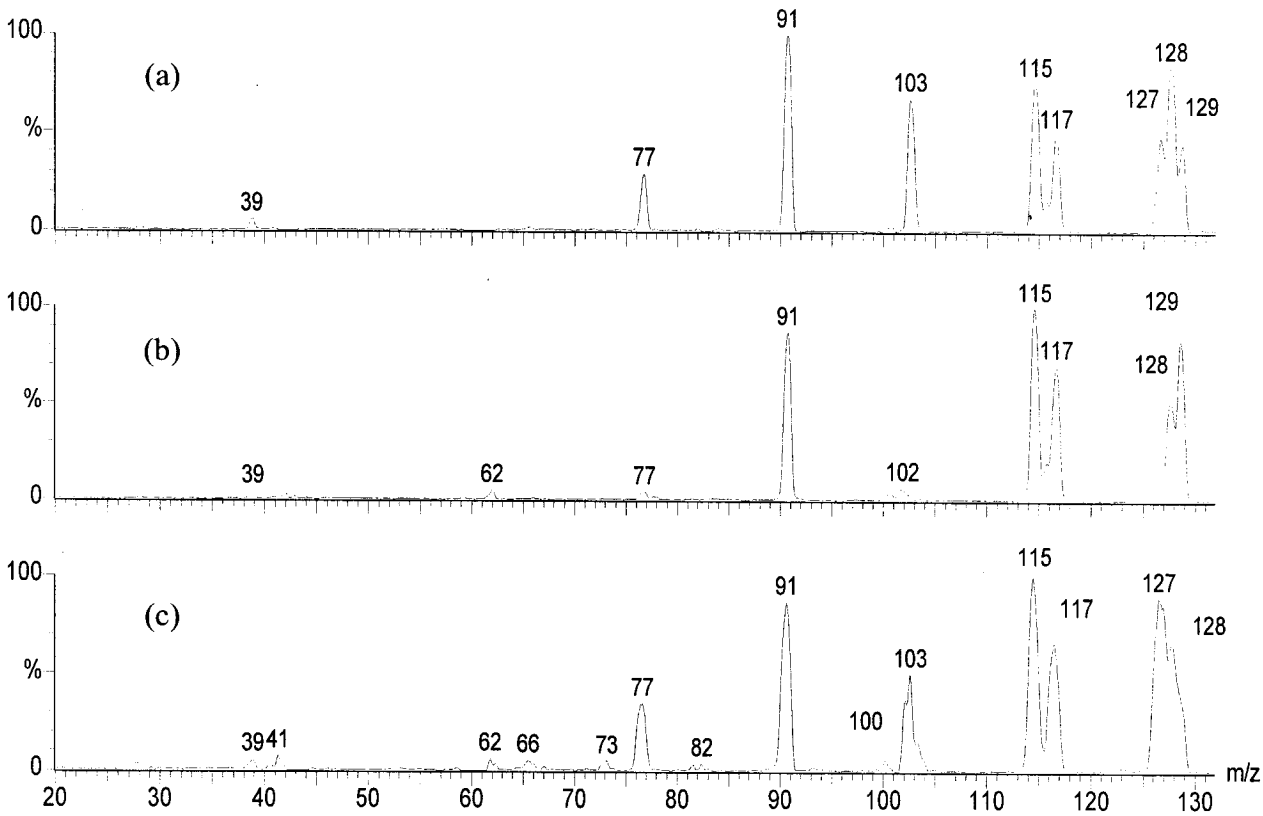

Figure 10. CID mass spectra of 3-methylquinoline (a), 8-methylquinoline (b), and 4-methylquinoline (c) at 25 eV. Ordinate scale has been expanded.

The collision energy dependence of this channel (Figure 11b) suggests a low energy threshold process governed by a tight transition state which may be more indicative of the loss of a neutral molecule such as CH_2NH. The fragment ion with *m/z* 103 is consistent with the loss of C_2H_3N (as was found for the methyl pyridines). Placing the methyl group on the benzene ring decreases the probability of this channel competing (as observed for ammonia loss). The ion at *m/z* 77 can be attributed to the phenyl cation, a process that again is hindered by the presence of the methyl group on the ring in protonated 8-methylquinoline.

Table 10. Relative peak intensities in the CID mass spectra of protonated methylquinolines at 25 eV.

m/z	Relative peak intensities		
	3-methylquinoline	4-methylquinoline	8-methylquinoline
129 $[MH-15]^+$	43	42	78
128 $[MH-16]^+$	81	66	52
127 $[MH-17]^+$	46	83	13
117 $[MH-27]^+$	43	54	69
115 $[MH-29]^+$	81	82	100
103 $[MH-41]^+$	81	73	24
101 $[MH-43]^+$	8	8	6
91 $[MH-53]^+$	100	100	92
77 $[MH-67]^+$	34	38	6
66 $[MH-78]^+$	2	4	1
62 $[MH-82]^+$	2	4	4
39 $[MH-105]^+$	5	4	5

(a)

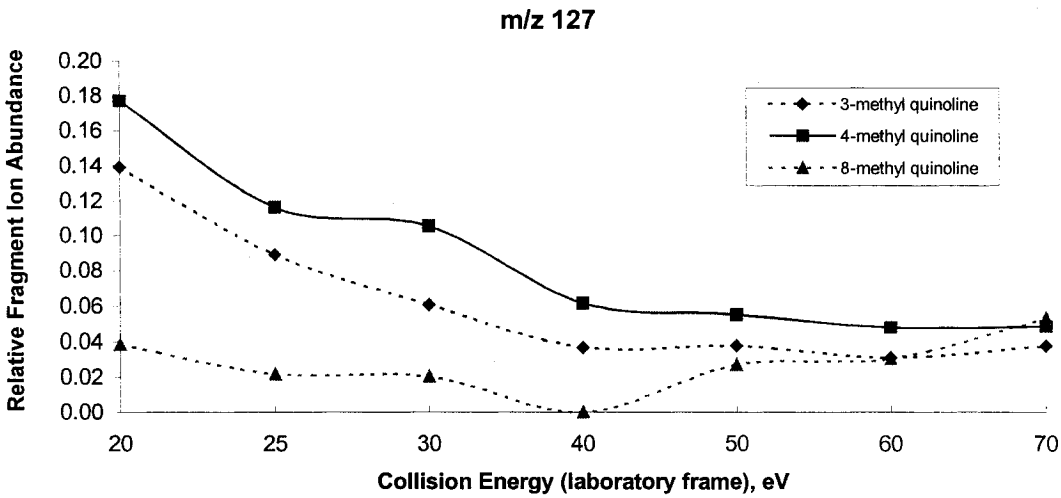

(b)

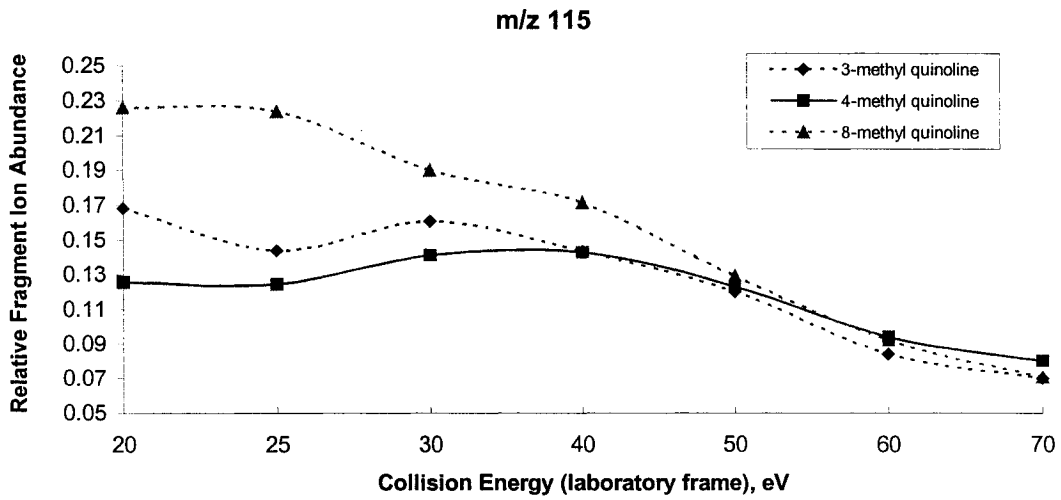

Figure 11. Energy dependence of fragment peaks of quinolines as a function of collision energy; *m/z* 127 (a) and *m/z* 115 (b).

3.3.9 Quinoline Derivatives: Dimethylquinolines

The CID mass spectra for protonated 2,4-dimethyl- and 2,7-dimethylquinoline (*m/z* 158) are presented in Figure 12 and summarized in Table 11. The 2,7- isomer, with a methyl on each ring, is distinguishable from the 2,4- isomer, which has both methyl groups on the pyridine ring. The 2,4-isomer favors methyl loss (*m/z* 143), whereas the loss of CH_4 is equally prominent for the 2,7-isomer (*m/z* 142). Unlike the pyridines, the collision energy dependence of both the methyl and methane loss channels are similar (Figure 13), suggesting that methyl loss is preceded by a rearrangement reaction such as hydrogen exchange.

Table 11. Relative peak intensities in the CID mass spectra of protonated dimethylquinolines at 25 eV.

m/z	Relative peak intensities	
	2,7-dimethylquinoline	2,4-dimethylquinoline
143 $[MH-15]^+$	77	100
142 $[MH-16]^+$	70	26
140 $[MH-18]^+$	4	5
131 $[MH-27]^+$	5	-
130 $[MH-28]^+$	4	5
117 $[MH-41]^+$	26	6
116 $[MH-42]^+$	15	7
115 $[MH-43]^+$	100	81
91 $[MH-67]^+$	65	41

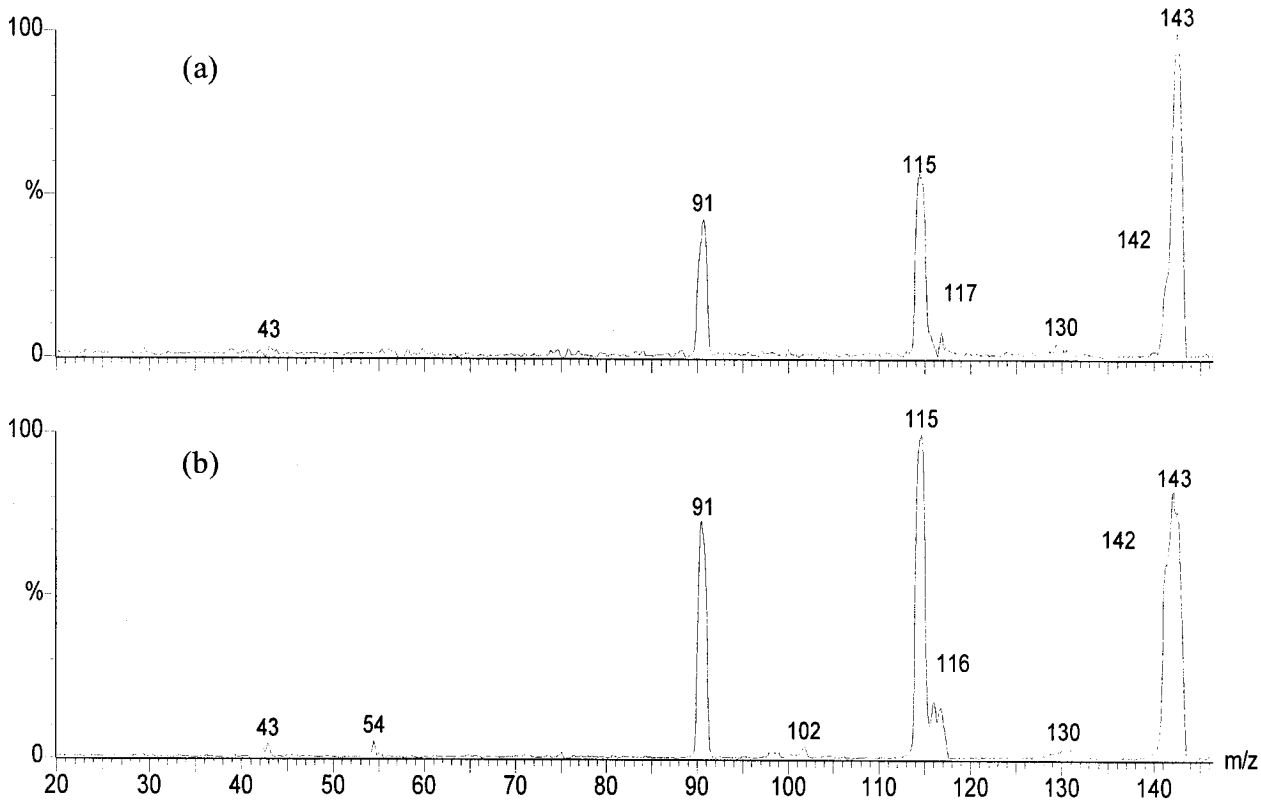

Figure 12. CID mass spectra of 2,4-dimethylquinoline (a) and 2,7-dimethylquinoline (b) at 25 eV. Ordinate scale has been expanded.

(a)

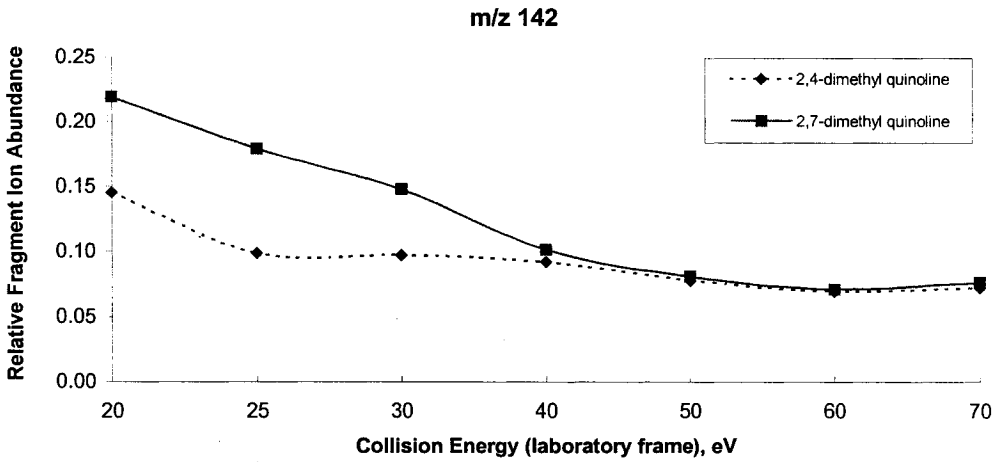

(b)

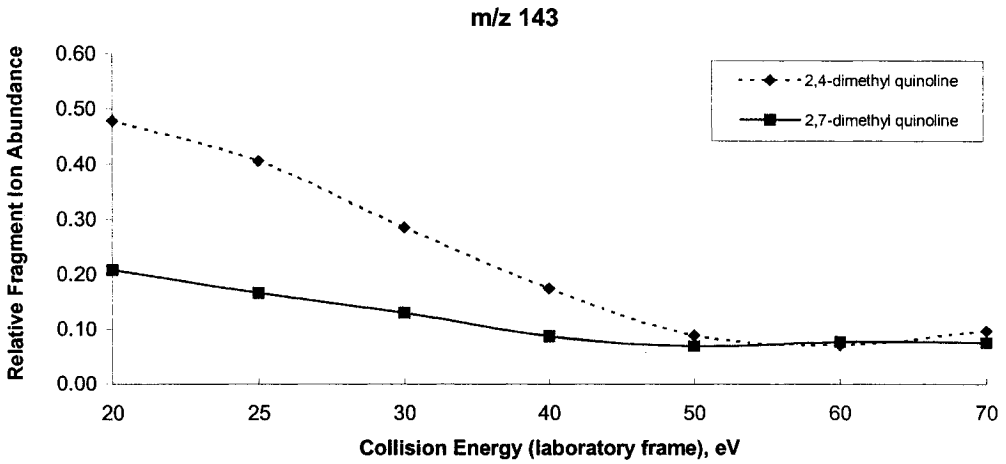

Figure 13. Energy dependence of fragment peaks of dimethyl quinolines as a function of collision energy; *m/z* 142 (a) and *m/z* 143 (b).

3.3.10 Quinoline Derivatives: Benzoquinolines

The CID mass spectra for protonated 2,3-benzoquinoline, 3,4-benzoquinoline and 7,8-benzoquinoline (*m/z* 180) are summarized in Table 12. All ions exhibited peaks at *m/z* 151, 152, and 153 in their spectra, corresponding to the loss of 29, 28, and 27 amu respectively. The loss of 28 amu is favored in the two protonated benzoquinolines that have a free C-H group adjacent to the protonated nitrogen atom, suggesting that loss of 28 amu is CH_2N. The 2,3-isomer strongly favored a loss of 27 amu which is likely due to loss of HCN. The 3,4- isomer stands alone as the only one producing a peak at *m/z* 128, due to loss of 52 amu. Similarly, a peak at *m/z* 107 was only seen in the spectrum for the 2,3-isomer.

Table 12. Relative peak intensities in the CID mass spectra of protonated benzoquinolines at 25 eV.

m/z	Relative peak intensities		
	2,3-benzoquinoline	3,4-benzoquinoline	7,8-benzoquinoline
153 $[MH-27]^+$	100	43	39
152 $[MH-28]^+$	65	100	100
151 $[MH-29]^+$	15	34	18
139 $[MH-41]^+$	6	39	4
128 $[MH-52]^+$	-	27	-
127 $[MH-53]^+$	6	17	8
107 $[MH-73]^+$	5	-	-

3.3.11 Indole Derivatives: Methylindoles

The CID mass spectra of protonated 1-, 2-, 3-, 5-, and 7-methylindole (*m/z* 132) are presented in Figure 14. The spectra are dominated by methyl loss (*m/z* 117), *m/z* 105 (-27) and *m/z* 91 (-41). The mass spectrum of protonated 1-methylindole is dominated by the loss of 41 amu to form *m/z* 91, distinguishing it from the other isomers. The presence of the methyl group on the nitrogen atom facilitating this channel leads to the conclusion that it is due to the loss of C_2H_3N rather than C_3H_5. Loss of 27 amu is enhanced when the methyl group is substituted on the benzene ring in protonated 5- and 7-methylindole (see Table 13). This supports the assignment of this channel to the loss of HCN. Loss of C_2H_3 should not have been blocked by placing the methyl group on the nitrogen atom as is evident in the mass spectrum of protonated 1-methylindole. Only protonated 5- and 7-methylindole exhibited a significant peak at *m/z* 71 corresponding to $[MH-61]^+$. It is difficult to distinguish between isomers having related methyl substitution, i.e., between protonated 2- and 3-methylindole and between protonated 5- and 7-methylindole.

Table 13. Relative peak intensities in the CID mass spectra of protonated methylindoles at 25 eV.

m/z	Relative peak intensities				
	1-methylindole	2-methylindole	3-methylindole	5-methylindole	7-methylindole
	52	100	100	100	100
105 $[MH-27]^+$	5	15	22	59	49
91 $[MH-41]^+$	100	5	14	6	14
90 $[MH-42]^+$	-	3	6	3	7
77 $[MH-55]^+$	3	2	5	4	-
71 $[MH-61]^+$	-	-	3	7	15
65 $[MH-67]^+$	5	-	-	1	-

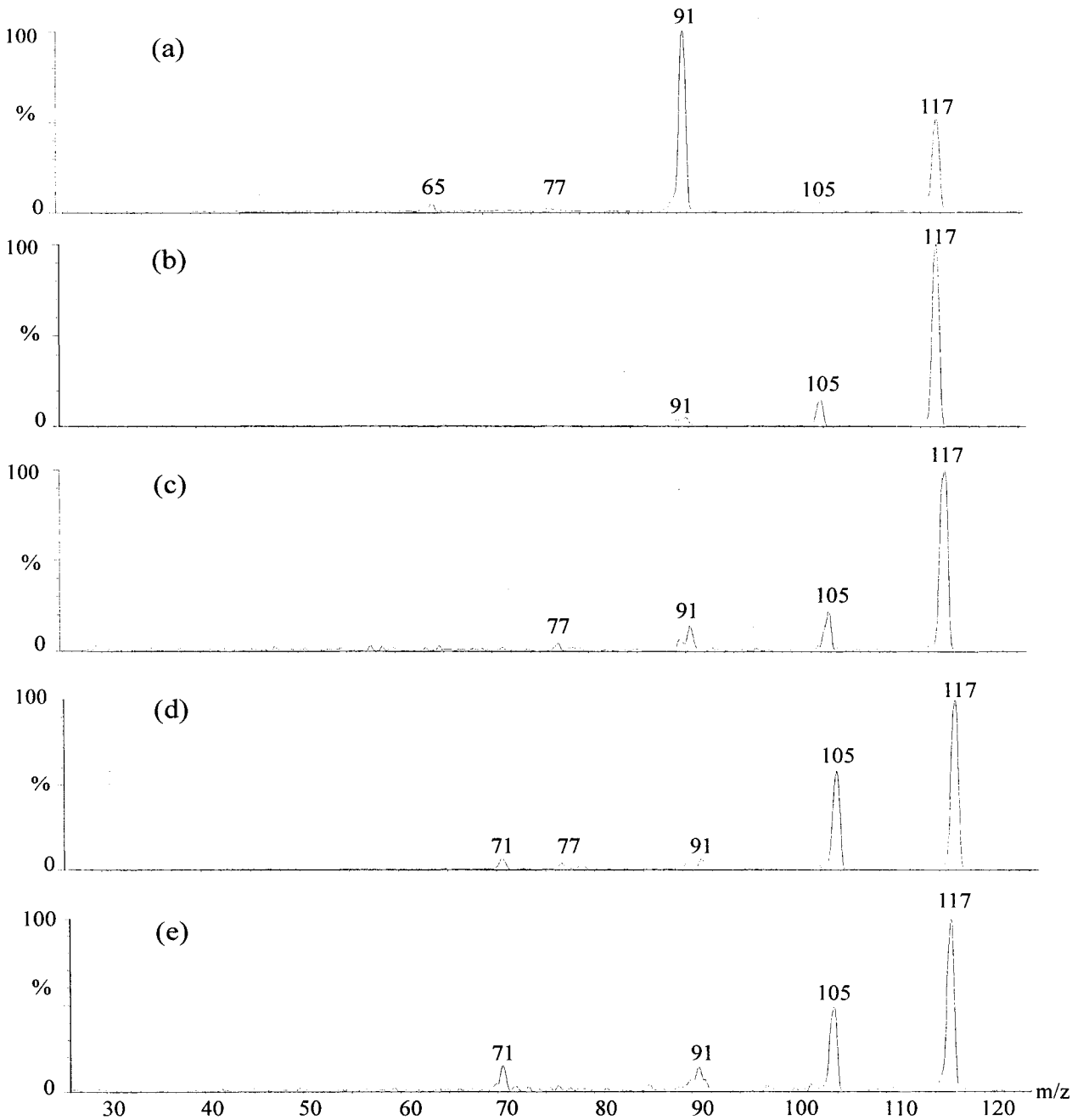

Figure 14. CID mass spectra of 1-methylindole (a), 2-methylindole (b), 3-methylindole (c), 5-methylindole (d), and 7-methyindole (e) at 25 eV. Ordinate scale has been expanded.

3.3.12 Indole Derivatives: Dimethylindoles

The CID mass spectra of protonated 1,2-dimethylindole and 2,3-dimethylindole (*m/z* 146) are summarized in Table 14. The mass spectra of both compounds are dominated by methyl loss (*m/z* 131) and loss of 41 (*m/z* 105). As for the mono-substituted indoles, substitution of a methyl group on the nitrogen atom facilitates the loss of 41 amu, again suggesting that a large portion of this signal is due to the loss of C_2H_3N. Protonated 2,3-dimethyl indole is distinguished by a significant peak at *m/z* 91 in its CID mass spectrum, which can be due to the loss of either C_3H_5N or C_4H_7. Methyl substitution on the ring enhances this channel suggesting that it is primarily due to the loss of the hydrocarbon, C_4H_7.

Table 14. Relative peak intensities in the CID mass spectra of protonated dimethylindoles at 25 eV.

m/z	Relative peak intensities	
	1,2-dimethylindole	2,3-dimethylindole
131 $[MH-15]^+$	100	100
117 $[MH-29]^+$	3	7
115 $[MH-31]^+$	1	1
105 $[MH-41]^+$	31	19
103 $[MH-43]^+$	2	-
91 $[MH-55]^+$	1	11
79 $[MH-67]^+$	2	2
77 $[MH-69]^+$	1	4

3.3.13 Carbazoles

The CID mass spectra of protonated 9-methyl-, 9-ethyl-, 9-phenyl-, 1,2,3,4-tetrahydro-, and 1,4,5,8,9-pentamethyl carbazole are summarized in Table 15. Unfortunately, there are no isomers amongst this group, but the data were included to enable a comparison with the other nitrogen containing compounds. The carbazole samples were initially fed into the electrospray using acetonitrile/water as mobile phase. However, this resulted in clogging of the capillary tip and poor mass spectra. Using acetonitrile/benzene as the mobile phase solved this problem and greatly improved the spectra.

Fragmentation of 9-methyl carbazole resulted in strong loss of methyl (*m/z* 167) followed by fragment peaks at *m/z* 153 (-29), *m/z* 152 (-30), *m/z* 151 (-31), and *m/z* 140 (-42). Loss of 29 amu is likely C_2H_5 or CH_3N as was seen in the ethyl pyridine spectra. The fragmentation pattern for 9-ethyl carbazole is similar to that of 9-methyl- except it contains an additional peak at *m/z* 180 due to the extra 14 amu. The mass spectrum is dominated by strong loss of the ethyl group (*m/z* 167) and loss of methane (*m/z* 180). For 9-phenyl carbazole, only a fragment ion peak corresponding to loss of the phenyl group is seen. It would be expected that the degree of fragmentation of any phenyl carbazole would be dependent on the position of the phenyl group, as was the case with the phenylpyridines. The fragmentation of 1,4,5,8,9-pentamethyl carbazole is dominated by loss of methyl group (*m/z* 223) and losses of 31 amu (*m/z* 207) and 32 amu (*m/z* 206).

Table 15. CID fragment peaks at 50 eV for substituted carbazoles.

Protonated Carbazole	Parent (*m/z*)	Fragment (*m/z*)	Neutral Loss	Relative Intensity
9-methyl-	182	167	15	100
		153	29	41
		152	30	22
		151	31	16
		140	42	10
		138	44	6
		128	54	8
		127	55	8
		114	68	5
9-ethyl-	196	180	16	80
		167	30	100
		154	42	16
		153	43	18
		140	56	5
		128	68	7
		126	70	4
		114	82	8
		113	83	6
9-phenyl-	244	166	78	100
1,4,5,8,9-pentamethyl-	238	223	15	100
		207	31	28
		206	32	16
		192	46	4
		180	58	2
		165	73	1
1,2,3,4-tetrahydro-	172	131	41	100
		130	42	76
		129	43	54
		77	95	52

The mass spectrum of 1,2,3,4-tetrahydro carbazole, is dominated by strong loss of 41, 42, and 43 amu (*m/z* 131, 132, and 133 respectively), followed by loss of 95 amu (*m/z* 77). The resonant positioning of the double bond in either the five member or the six member ring may be partly responsible for this series of peaks. In the methylpyridine spectra, the ion at *m/z* 42 was attributed to either CH_3CNH^+ or $C_3H_6^+$ while the ion at *m/z* 41 was confirmed to be $C_3H_5^+$. It is possible that all three of these ions are present here due to a simple alpha cleavage occurring in one of the rings.

3.4 Conclusions

Electrospray ionization tandem mass spectrometry has been used to differentiate between a large variety of nitrogen-containing aromatic compounds. Isotopic labeling has been used to help identify fragmentation products, as has the collision energy dependence of the CID mass spectra. These results may be useful in identifying new biomarkers for tracking the fate of crude oil contamination in the environment.

3.5 References

1. Kropp, K.G.; Fedorak, P.M. A review of the occurrence, toxicity, and biodegradation of condensed thiophenes found in petroleum. *Can. J. Microbiol.* **1998**, *44*, 605-622.
2. Law, S.A.; Diamond, M.L.; Helm, P.A.; Jantunen, L.M.; Alaee, M. Factors affecting the occurrence and enantiomeric degradation of hexachlorocyclohexane isomers in northern and temperate aquatic systems. *Environ. Toxicol. Chem.* **2001**, *20* 2690-2698.
3. Rainio, A.; Vahvaselka, T.; Suomalainen, T.; Laakso, S. Reduction of linoleic acid inhibition in production of conjugaed linoleic acid by *Propionibacterium freudenreichii ssp. shermanii*. *Can. J. Microbiol.* **2001**, *47*, 735-740.
4. Swisher, R.D. *Surfactant Biodegradation*, 2nd Edition, Surfactant Science Series, Marcel Dekker, Inc.: New York, **1987**.
5. Wang, Z.; Fingas, M.; Li, K. Fractionation of a light crude oil and identification and quantification of aliphatic, aromatic, and biomarker compounds by GC-FID and GC-MS, Part II. *J.Chrom. Sci.* **1994**, *32*, 367-382.
6. Fayad, N.M.; Overton, E. A unique degradation pattern of the oil spilled during the 1991 gulf war. *Mar. Pollut. Bull.* **1995**, *30*, 239-246.
7. Chiarenzelli, J.; Scrufata, R.; Wunderlich, M.; Rafferty, D.; Jensen, K.; Oenga, G.; Roberts, R.; Pagano, J. Photodecomposition of PCBs absorbed on sediment and industrial waste: Implications for photocatalytic treatment of contaminated solids. *Chemosphere* **1995**, *31*, 3259-3272.
8. Wang, Z.; Fingas, M. Developments in the analysis of petroleum hydrocarbons in oils,

petroleum products and oil-spill related environmental samples by gas chromatography. *J. Chromatogr. A* **1997**, *774*, 51-78.

9. Wang, Z.; Fingas, M.; Landriault, M.; Sigouin, L.; Yuepeng, F.; Mullin, J. Using systematic and comparative analytical data to identify the source of an unknown oil on contaminated birds. *J. Chromatogr. A* **1997**, *775*, 251-265.

10. Ignatiadis, I., Kuroki, M., and Arpino, P.J. Identification of carbazole derivatives in a hydrotreated coker gas oil by gas chromatography and gas chromatography-mass spectrometry. *J. Chromatogr.* **1986**, *366*, 251-260.

11. Li, M., Larter, S.R., and Stoddart, D. Liquid chromatographic separation schemes for pyrrole and pyridine nitrogen aromatic heterocycle fractions from crude oils suitable for rapid characterization of geochemical samples. *Anal. Chem.* **1992**, *64*, 1337-1344.

12. Snyder, L.R. and Buell, B.E. Nitrogen and oxygen compound types in petroleum, a general separation scheme. *Anal. Chem.* **1968**, *40*, 1295-1302.

13. Later, D.W., Lee, M.L., Bartle, K.D. and Vassilaros, D.L. Chemical class separation and characterization of organic compounds in synthetic fuels. *Anal. Chem.* **1981**, *53*, 1612-1620.

14. Schiller, J.E., and Mathiason, D.R. Separation method for coal-derived solids and heavy liquids. *Anal. Chem.* **1977**, *49*, 1225-1228.

15. Ford C.D., Holmes, S.A., Thompson, L.F., and Latham, D.R. Separation of nitrogen compound types from hydrotreated shale oil products by adsorption chromatography on basic and neutral alumina. *Anal. Chem.* **1981**, *53*, 831-836.

16. Vairamani, M.; Prabhakar, S.; Raju, N.P.; Rao, G.K.V. Acetone chemical ionization

studies. VIII: Pyridine derivatives. *Eur. Mass Spectrom.* **1995**, *1*,539-543.

17. Sakurai, H., and Jennings, K. R. A. A study of the structures of decomposing and non-decomposing $[C_4H_5N]^{+\cdot}$ ions formed from different neutral species. *Org. Mass Spectrom.* **1981**, *16*, 393.

18. Maquestiau, A.; Van Haverbeke, Y.; Flammang, R.; Mispreuve, H. Chemical ionization of hydroxypyridine structures. *Bull. Soc. Chim. Belg.* **1979**, 88, 395-414.

19. Daishima, S.; Yoshio, I. Chemical ionization mass spectra of nitrogen aromatics. *Shitsuryo Bunseki*, **983**, 31(4), 281-7.

20. Sorrilha, Ana Elisa P.M., Gozzo, Fabio C., Pimpim, Regina S., and Eberlin, Marcos N. Multiple stage pentaquadrupole mass spectrometry for generation and characterization of gas-phase ionic species. The case of the $PyC_2H_5^{+\cdot}$ isomers. *J. Am. Soc. Mass Spectrom.* **1996**, *7*, 1126-1137.

21. Maquestiau, A.; Van Haverbeke, Y.; De Meyer, C.; Katritzky, A.R.; Cook, M.J., and Page, A.D. Mise en évidence des tautomères énoliques des hydroxypyridines dans la source du spectromètre de masse. *Can. J. Chem.* **1975**, Vol 53, 490-496.

22. Perrin, D.D.; Dempsey, B; and Serjeant, E.P. *pKa Prediction for Organic Acids and Bases*; Chapman and Hall in association with Methuen, Inc.: New York, **1981**.

23. Van Thuijl, J., Van Houte, J.J., Maquestiau, A., Flammang, R., De Meyer, C. The formation and structure of $[C_2H_3N]^{+\cdot}$ radical cations. *Org. Mass Spectrom.* **1977**, *12*, 196-199.

24. Busch, K. L.; Glish, G. L.; McLuckey, S. A. *Mass Spectrometry/Mass Spectrometry*; VCH Publishers: New York, **1988**.

25. Baer, T.; Hase, W. L. *Unimolecular Reaction Dynamics, Theory and Experiments*; Oxford University Press: New York, **1996**.

Chapter 4 - Analysis of Oil Resins Using Electrospray-Ionization Tandem Mass Spectrometry

4.1 Introduction

Crude oil is a complex mixture that is known to contain small quantities of nitrogen, sulfur, and oxygen containing compounds. Many of these polar chemicals can be found in the heavier asphaltene and resin fractions of oils. Use of the popular SARA fractionation procedure allows oils to be separated into fractions containing Saturates, Aromatics, Resins, and Asphaltenes. This has enabled individual and chemical class identifications of the many constituents present in oils worldwide.

The polar resin fraction of an oil is usually a dark brown to black ductile semisolid. Its complexity and physical properties make it difficult for any type of compound class separation let alone individual chemical identification. Despite this difficulty, resins have been studied on numerous occasions and reported to contain many different compounds like sulfoxides, sulfides, sulfones, amides, thiophenes, pyridines, quinolines, and carbazoles [1-2]. The methods employed for the analyses of resins have varied. There are several reports on the use of structural FTIR [3-6] and one involving X-ray absorption near-edge structure (XANES) spectroscopy [2]. Others include nuclear magnetic resonance [6,7], mass spectrometry [6,8], and high performance liquid chromatography-flame ionization detection [9].

Electrospray ionization mass spectrometry is becoming a common method for the analysis of petroleum based chemicals [10-14] and oilfield additives [15-16]. This is due to the ease with which one can couple HPLC to mass spectrometry and conduct analyses of polar, ionic, and neutral compounds dissolved in simple solvents. In the present study, ESI-MS and tandem mass spectrometry have been used for the analysis of the polar resin fraction from several crude oils, fuel oils, and diesel.

4.2 Experimental Section

4.2.1 Resin Samples

Polar resin samples prepared by SARA fractionation [17] were obtained from the Emergencies Science and Technology Division of Environment Canada in Ottawa. The resins were extracted from oil samples of Alberta Sweet Mixed Blend (ASMB), Mars, Alaskan Northslope, Hibernia, Maui, Arabian Heavy, and Tchat. Resin samples from the petroleum products Diesel, Heavy Fuel Oil (HFO 6303), and Fuel Oil #5 were also obtained along with weathered samples of all resins, except ASMB. The origin of each resin sample can be found in Table 16.

Table 16. A list of the resins studied and their origins.

Resin	Origin	Notes
Maui	Crude oil	From Shell Todd Oil Services Ltd., New Zealand
Tchatamba (Tchat)	Crude oil	From Marathon Oil, Gabon (Africa)
Alaskan Northslope (ANS)	Crude oil blend	Drawn off the TAPS pipeline in Valdez, Alaska, U.S.A.
Arabian Heavy	Crude oil blend	From Saudi Arabia; "heavy" indicates a commercial (density) grade oil
Hibernia	Crude oil	From Hibernia, offshore Newfoundland, Canada
Mars	Crude oil	From Shell, offshore Gulf of Mexico, U.S.A.
Alberta Sweet Mix Blend (ASMB)	Crude oil blend	From ESSO, Alberta, Canada
Fuel Oil #5	Refined oil product	From U.S. Dept. Int., M.M.S., OHMSETT, New Jersey, U.S.A.; for ship fuel and power generation
HFO 6303	Refined oil product	From Imperial Oil Ltd, Nova Scotia, Canada; Heavy Fuel Oil (HFO) for ship fuel and power generation; also known as Bunker C, Marine Boiler Fuel, and Land Bunker
Diesel	Refined oil product	From local retailer Stinson's Gas, Ontario, Canada; also known as "Summer Diesel"

Stock solutions of the resin in the range 4-7 g resin/L were prepared using various solvents. After addition of solvent, the samples were shaken vigorously for two minutes and allowed to stand overnight. All were orange-brown in colour and some had small amounts of undissolved resin remaining on the sides of the vial. Subsamples with concentrations of ~ 1 g

resin/L were later prepared and were spiked with a conductivity additive as needed. These will be described in more detail in the results sections that follow. All subsamples formed clear yellow-orange solutions and appeared to have no undissolved matter.

Experiments were also conducted with resins prepared in perdeuterated acetone obtained from C/D/N Isotopes Inc. (Point-Claire, QC), 99% purity, 99.5% isotopic enrichment. For these experiments, the mobile phase was matched to that of the sample solvent. If needed, samples were spiked with 0.4% acetic acid (v/v) to increase the conductivity.

4.3 Results and Discussion

4.3.1 Crude Oil Resins

The first task involved finding a solvent system that could adequately dissolve some of the polar resin compounds and which could be used with an electrospray mass spectrometer. In early experiments, a solvent of composition 50/50 acetonitrile/benzene coupled with the same mobile phase worked well. Acetic acid (0.4 % v/v) was added to the samples to increase the conductivity. Using this system and subtracting the mobile phase, the mass spectrum from an ASMB sample was found to contain numerous compounds in the range *m/z* 20-600 with the highest peak at *m/z* 312 (Figure 15a). A distinct "hump" is seen in the range *m/z* 200-600 with incremental peaks differing by two mass units. This is assumed to be the result of a difference in saturation between compounds of neighbouring *m/z*.

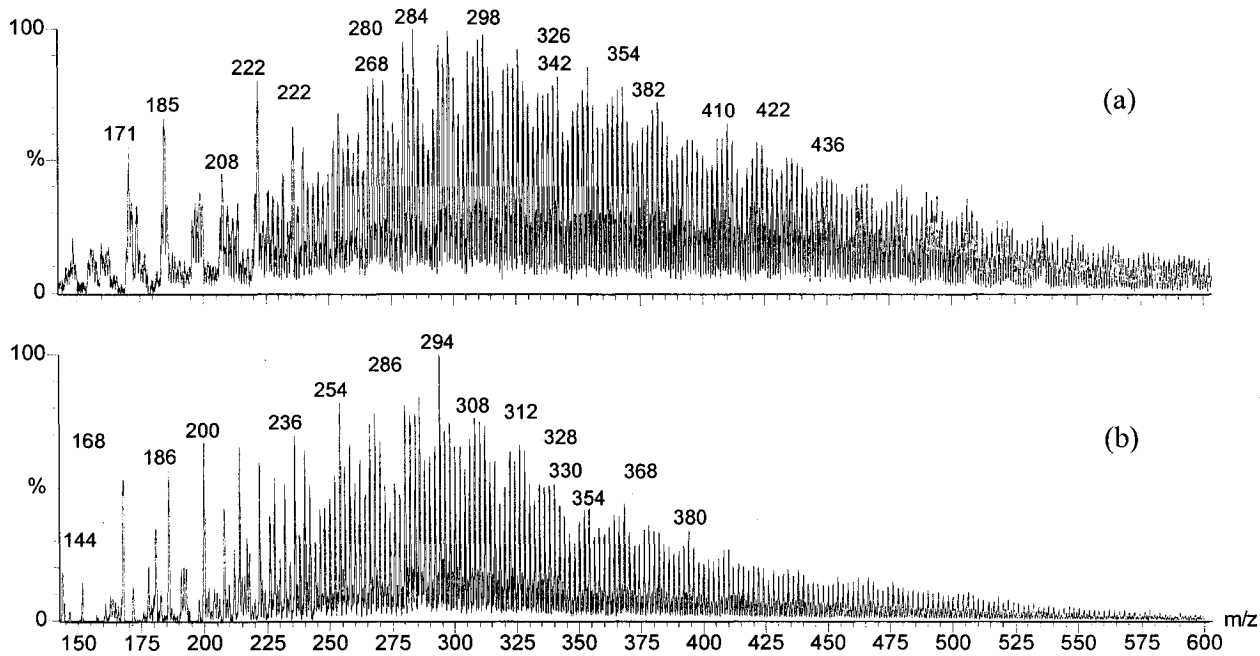

Figure 15. Mass spectra of ASMB resin obtained using 50/50 acetonitrile/benzene mobile phase (a) and acetone mobile phase (b). Ordinate scale has been expanded.

Also observed were periodic peaks that differed by 14 mass units which were attributed to the presence of an additional CH_2 group on an alkyl chain. Zhan and Fenn [10] encountered the same phenomena in their ESI spectra of crude oil. With the two mass unit difference, approximately 150 compounds are present in the observed resin mass spectrum hump. Since all observed peaks are of even mass, the unprotonated compounds are of odd mass and may contain an alkyl or heterocyclic nitrogen atom.

In subsequent experiments, acetone was used as both the sample solvent and mobile phase and acetic acid (0.4% v/v) added to increase conductivity. The mass spectrum for an ASMB sample with this system was similar to that obtained in the acetonitrile/benzene mobile phase (Figure 15b). Acetone proved to be efficient in extracting a similar amount of polar material from the resins as did the other solvents, and produced consistent spectra. Acetic acid (0.4 % v/v) was used periodically to increase the conductivity, but good spectra could be obtained without it. Based on the results of these studies, it was decided that acetone would be used as both the sample solvent and mobile phase for the remaining resins.

The mass spectra obtained for the other six oil resins were similar to that for ASMB, with a main distribution of peaks in the range *m/z* 200-600 (Figure 16, a-g). All spectra displayed the same pattern of incremental peaks differing by two mass units and distinct tall peaks 14 mass units apart. These spectra differed slightly by the presence of low molecular weight compounds in the *m/z* 75-200 range.

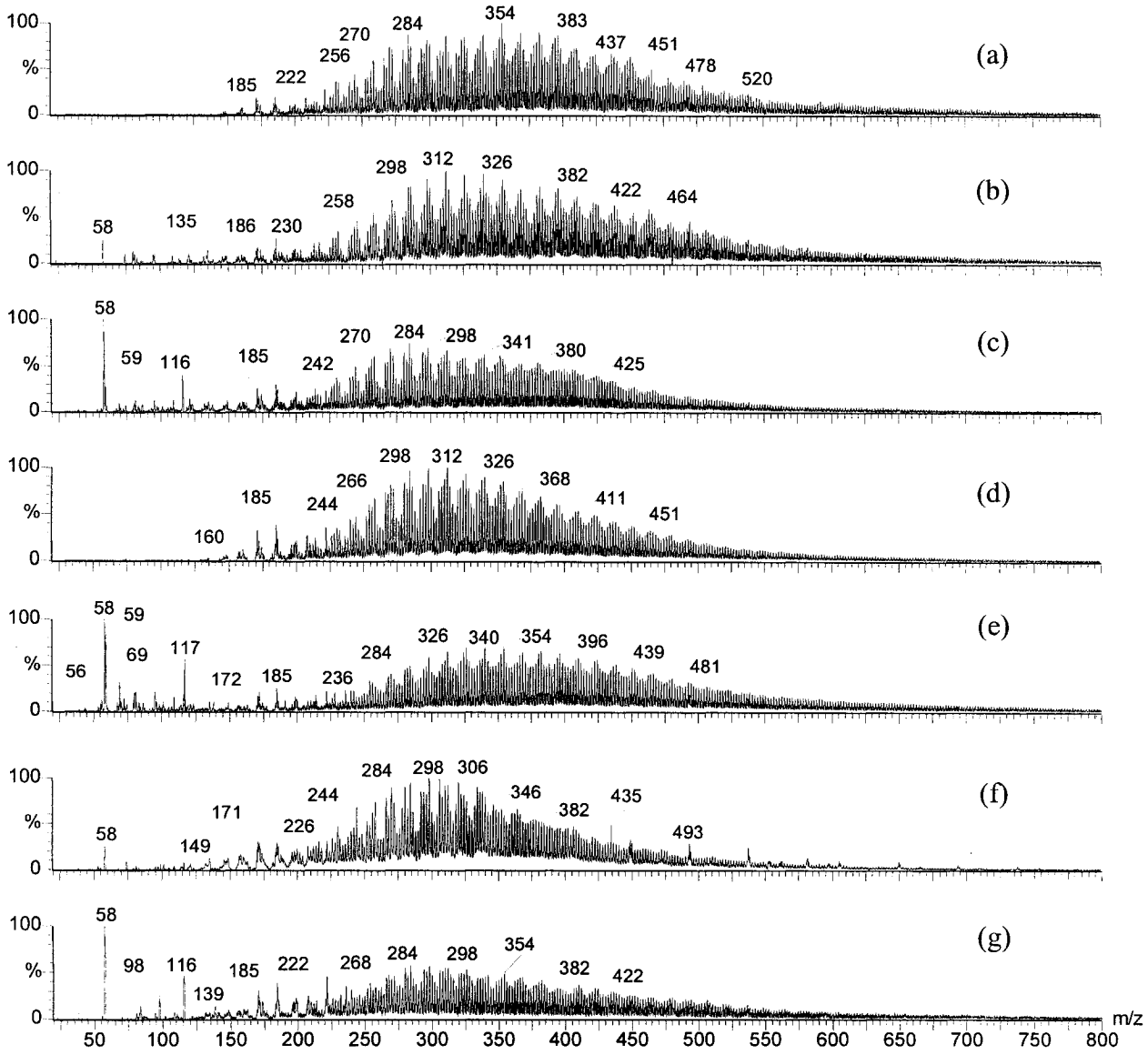

Figure 16. Mass spectra of crude oil resins: Hibernia (a), Mars (b), Tchat (c), Alaskan Northslope (d), Arabian Heavy (e), Maui (f), and ASMB (g).

The fragmentation of *m/z* 298 from the ASMB resin at 80 eV collision energy is presented in Figure 17 (a) along with a list of the fragments ions in Table 17. A series of ions separated by 14 mass units is observed. This is similar to a hydrocarbon cracking pattern in the mass spectrometry of alkanes. The fragment peaks in the spectrum end at *m/z* 142 giving a total loss of 156 mass units from the main compound. The *m/z* 142 peak is probably the main ring structure of the compound and very stable since it is not susceptible to any further dissociation. It is presumed to contain a heteroatom like nitrogen which enables it to be protonated and detected using ESI-MS.

An investigation of the two mass unit increment observed in all resin mass spectra was conducted by performing collision experiments on the *m/z* trio 294-296-298. The fragmentation pattern should indicate whether or not the peaks are the result of increasing saturation in a ring or alkyl chain. If a double bond is present in an alkyl chain, it would be expected to exhibit a unique fragmentation pattern differing from that of the next higher or lower *m/z* compound. However, if present in a ring system the fragmentation pattern would be similar to that for the next higher or lower *m/z* compound, with the fragment ion peaks being two mass units higher or lower. The fragmentation patterns of *m/z* 294, 296, and 298 as presented in the ASMB spectra are in Table 17. The pattern for *m/z* 296 was similar to that of *m/z* 294, except that its fragment peaks were two mass units higher. The same was observed for *m/z* 298 when compared to *m/z* 296. It can be concluded from this trio that the two unit incremental difference is the result of increasing saturation in a ring system, and not in an alkyl chain.

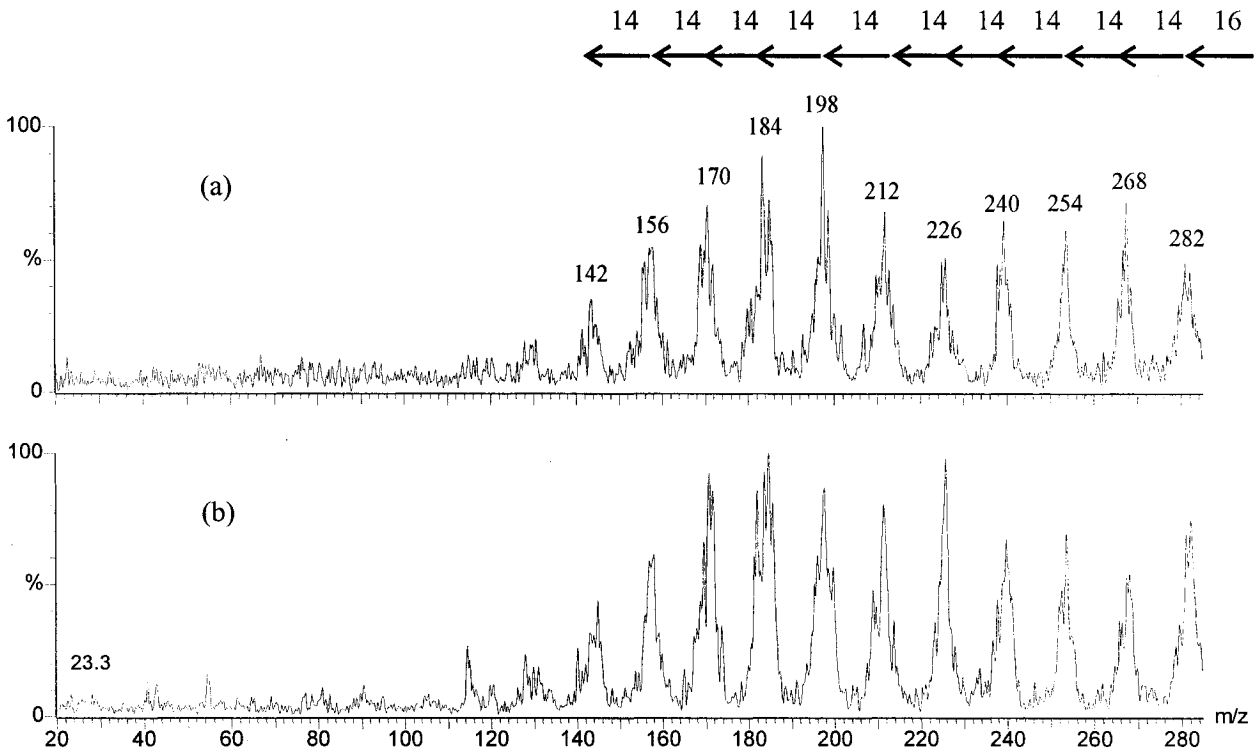

Figure 17. CID mass spectra of ASMB compound *m/z* 298 obtained with acetone as the mobile phase (a) and acetone d6 as mobile (b). Spectra were obtained using a collision energy of 100 eV. Ordinate scale has been expanded to enhance fragment ion peaks.

Table 17. Fragment ions (*m/z*) and neutral losses between fragments for resin compounds *m/z* 294, 296, and 298 at 80 eV collision energy.

Parent (*m/z*)	Fragment Ion (*m/z*)	Mass Difference Between Fragments
294	278	16
	264	14
	250	14
	236	14
	222	14
	208	14
	194	14
	180	14
	166	14
	152	14
296	280	16
	266	14
	252	14
	238	14
	224	14
	210	14
	196	14
	182	14
	170	14
	156	14
298	282	16
	268	14
	254	14
	240	14
	226	14
	212	14
	198	14
	184	14
	170	14
	156	14

The collision experiments on the ASMB resin revealed a reoccurring *m/z* 58 peak in all spectra. To determine if this was due to the solvent system (acetone), experiments were conducted using isotopically labelled acetone d_6 as both the carrier and sample solvent. After performing collision experiments on the same *m/z* compounds in each solvent, it was discovered that the mass losses were in fact authentic and not due to loss of acetone. No shift in mass for the *m/z* 58 fragment peak was observed during the acetone d_6 CID experiments (Figure 17b).

The fragmentation of the trio *m/z* 240-254-268 from the ASMB resin was studied at a collision energy of 50 eV to determine if these compounds were related. The spectra of this grouping revealed a similar pattern (Figure 18) with the fragment ion peaks from *m/z* 240 being present in the spectra for *m/z* 254, and the same relationship being observed between *m/z* 254 and *m/z* 268. It is therefore reasonable to conclude that this trio is comprised of compounds from the same chemical class.

After obtaining CID mass spectra for several resin compounds, a comparison was made with those of the pyridines, indoles, quinolines and carbazoles that were presented earlier. Although higher cone and collision energies were used to obtain the resin CID mass spectra, the study on 3-methylpyridine (presented earlier) demonstrated that these parameters affect relative fragment ion intensity and not the actual fragment ion pattern. Therefore, a comparison of the resin CID mass spectra with the standards is possible. The only class of compounds that yielded similar results were carbazoles. Indeed, previous researchers have identified carbazoles in resins and other fossil fuels [6, 19, 20]. The fragmentation results were presented earlier in Table 15.

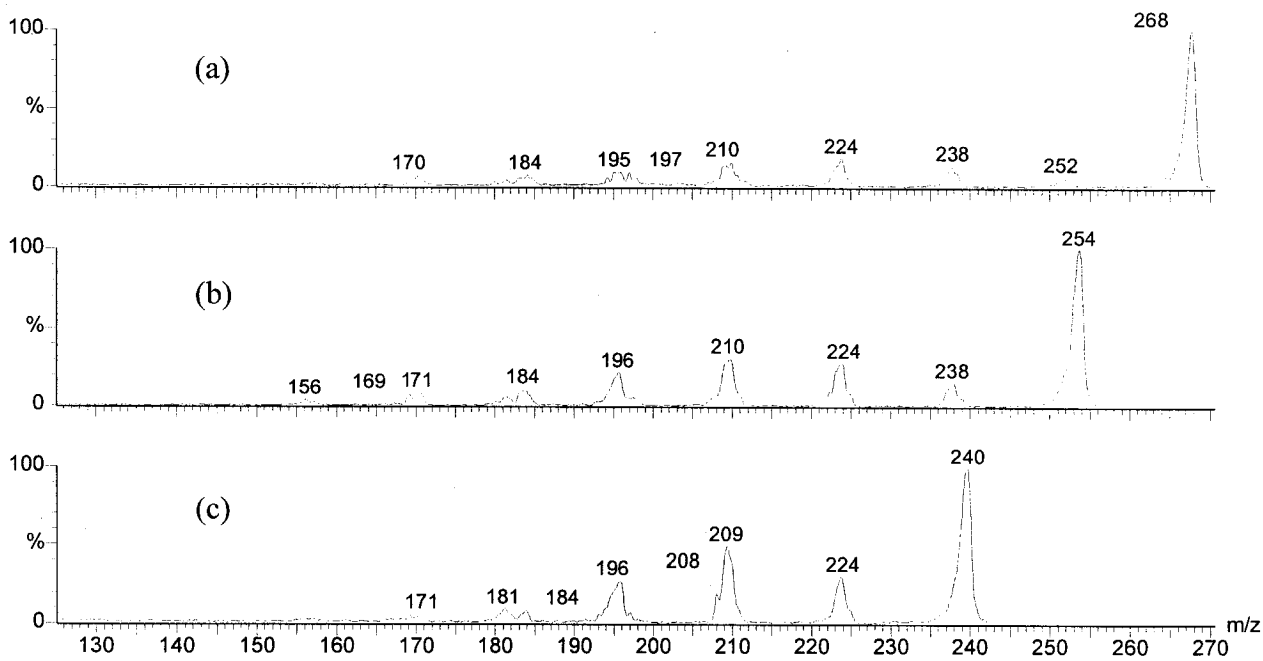

Figure 18. CID mass spectra of ASMB compounds *m/z* 268 (a), *m/z* 254 (b), and *m/z* 240 (c).

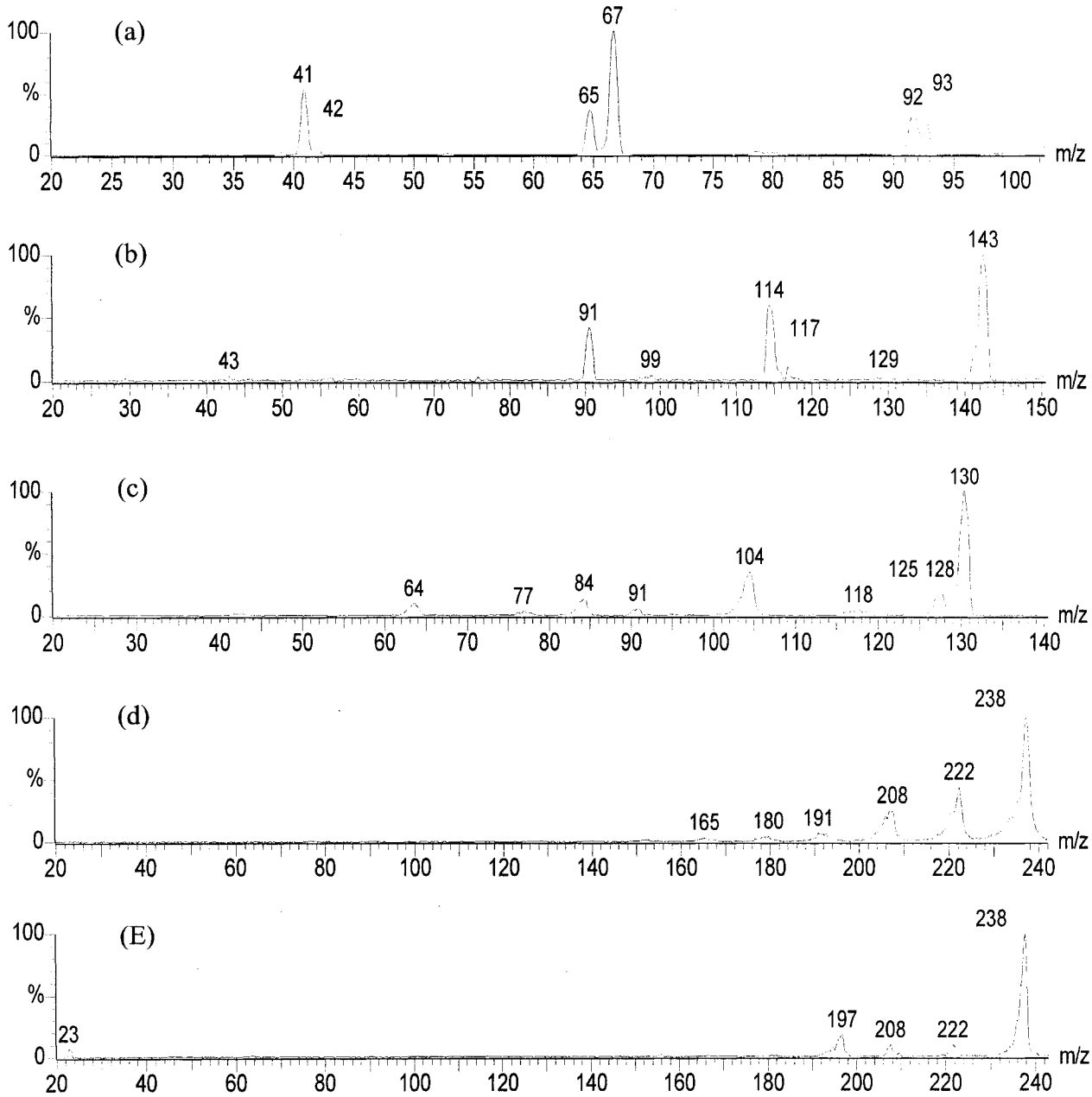

Figure 19. CID mass spectra at 25 eV (unless otherwise indicated) of 2,6-dimethylpyridine (a), 2,4-dimethylquinoline (b), 2,3-dimethylindole (c), 1,4,5,8,9-pentamethyl carbazole at 50 eV(d), and ASMB *m/z* 238 at 50 eV(e). Ordinate scales of a, b, and c have been expanded.

The CID mass spectrum for protonated 1,4,5,8,9-pentamethyl carbazole (*m/z* 238) is very similar to that obtained for ASMB resin *m/z* 238 (Figure 19) at varying collision energies. Secondly, Figure 20 shows that the fragment ion peaks in the CID mass spectrum of 9-methyl carbazole are all present in the CID mass spectrum of 9-ethyl carbazole which is 14 mass units larger. This same trend was observed in the fragmentation patterns of resin compounds *m/z* 240, 254 and 268 (discussed earlier). From these results, it is reasonable to conclude that the protonated resin constituents studied here are most likely carbazoles.

4.3.2 Fuel Oil Resins

Two samples of fuel oil were studied and the mass spectra for these oils are presented in Figure 21. Immediately, one can see that the mass spectrum for Heavy Fuel Oil 6303 (HFO) is quite unique with a narrow distribution of low molecular weight compounds, encompassing the range *m/z* 100-400. Unlike the crude oil mass spectra, a low intensity band of peaks continues from *m/z* 400 to 1000, forming a slight hump between *m/z* 600 and 900. The mass spectrum of Fuel Oil #5 could easily be mistaken for one of the crude oils that were studied as it contains the same "hump" of peaks in the *m/z* 200-500 region which slowly tapers off toward *m/z* 900. Both fuel oils contain the same ions in the *m/z* 100-400 region, but show spectral differences in the abundances (peak heights) of these ions. While HFO appears to contain more higher molecular weight material as evidenced by the peaks in the *m/z* 600-1000 range, a determination of the average number molecular weight (Mn) for the *m/z* 220-750 regions of these oils revealed similar values; HFO, Mn = 405, Fuel Oil #5, Mn = 404.

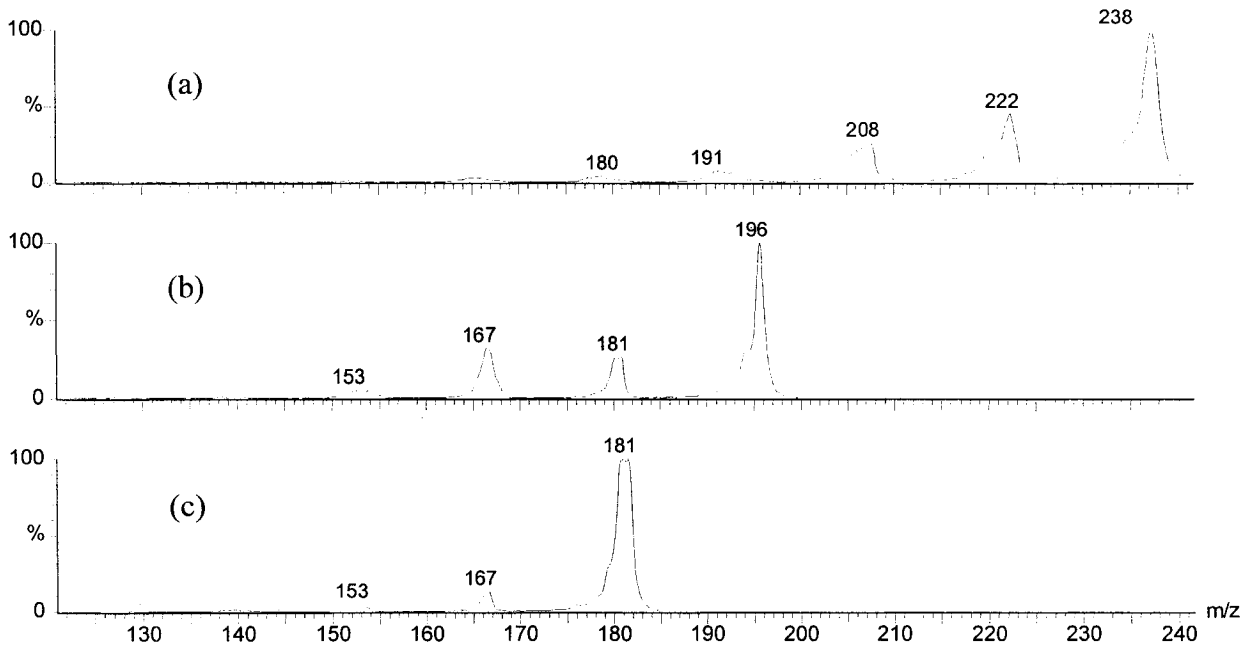

Figure 20. CID mass spectra of carbazoles: 1,4,5,8,9-Pentamethyl- (a), 9-Ethyl- (b), and 9-Methyl- (c).

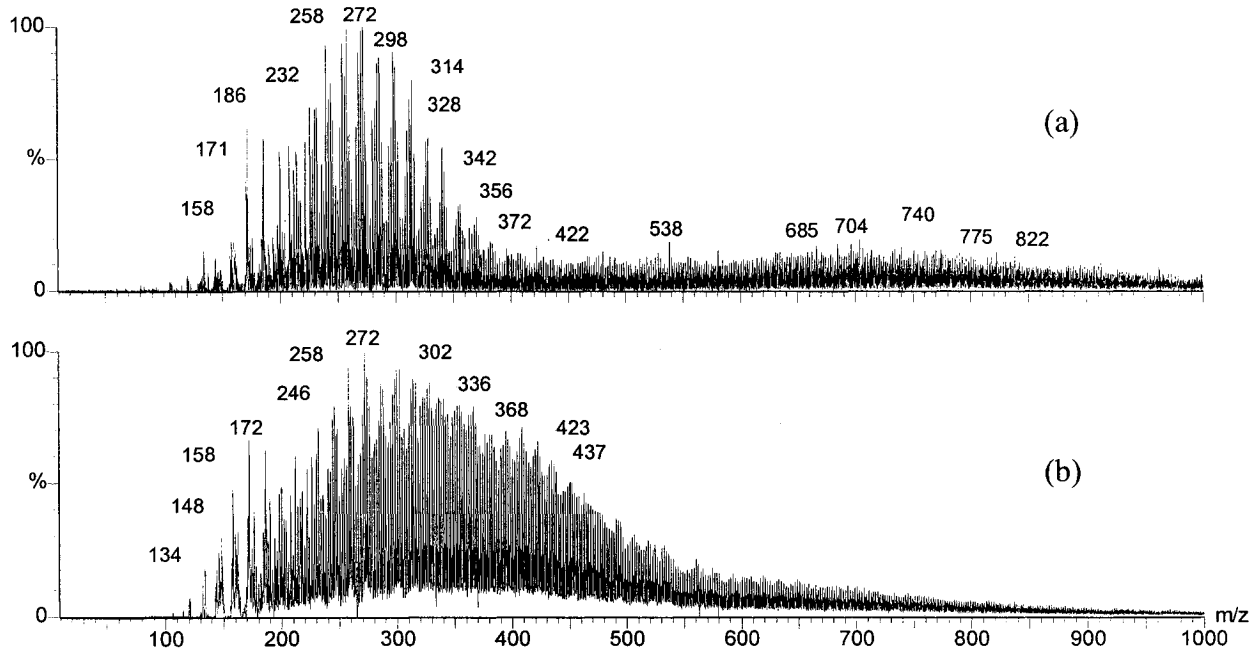

Figure 21. Mass spectra of Fuel Oils: HFO 6303 (a), and Fuel Oil #5 (b).

4.3.3 Diesel Resins

The mass spectrum for a sample of "summer diesel" was found to contain significantly fewer peaks than any of the other resins. All of these peaks occupied the *m/z* 60-340 range (see Figure 22) with *m/z* 172 being the most abundant. The mass spectrum is less congested than those of the oil resins but has the same pattern of periodic peaks 14 mass units apart. CID experiments were conducted on several ions in the diesel sample to see if their structure could be determined. A summary of the data is presented in Table 18 (a,b). The first CID experiments were conducted on two odd *m/z* ions, 95 and 135, which are likely oxygen or sulphur compounds. The ions fragmented in a similar fashion indicating that they may be related. The other four substances are assumed to be nitrogen containing aromatics based on the even *m/z* for the protonated parent molecules. Like before, the results were compared with the CID mass spectra of the pyridine, carbazole, indole and quinoline compounds. The mass spectrum of *m/z* 158 compared very well with the mass spectra for 2,7-, and 2,4-dimethylquinoline (Figure 23) and indeed has a *m/z* 142:143 consistent with the latter. The *m/z* 172 and *m/z* 186 ions display similar fragmentation patterns but the mass spectra are not consistent with those of the carbazoles, pyridines, quinolines, or indoles. The *m/z* 200 ion has the same fragmentation pattern as some of the ASMB compounds presented earlier and is likely a carbazole.

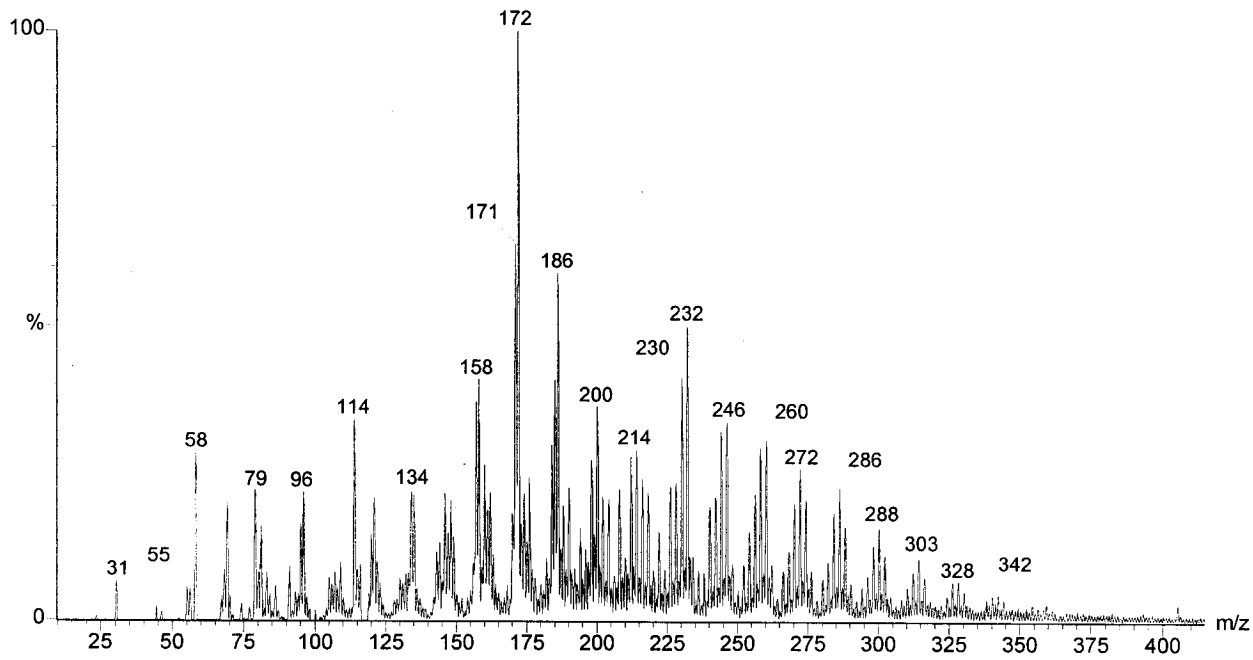

Figure 22. Mass spectrum of a sample of "summer diesel."

Table 18 (a). CID fragment ion peaks and neutral losses in mass spectra of diesel compounds at 30 eV.

Parent (*m/z*)	Fragment (*m/z*)	Neutral Loss
95	80	15
	79	16
	77	18
	67	28
	65	30
	55	40
	53	42
	51	44
	43	52
	41	54
	39	56
	29	66
	27	68
135	120	15
	107	28
	106	29
	93	42
	91	44
	80	55
	79	56
	77	58
	65	70
	59	76
	55	80
	41	94
158	143	15
	142	16
	130	28
	116	42
	115	43
	91	67

Table 18 (b). CID fragment ion peaks and neutral losses in mass spectra of diesel compounds at 30 eV.

Parent (*m/z*)	Fragment (*m/z*)	Neutral Loss
172	157	15
	142	30
	129	43
	116	56
	114	58
	91	81
186	171	15
	157	29
	156	30
	143	43
	130	56
	115	71
	105	81
	91	95
200	185	15
	171	29
	157	43
	142	58

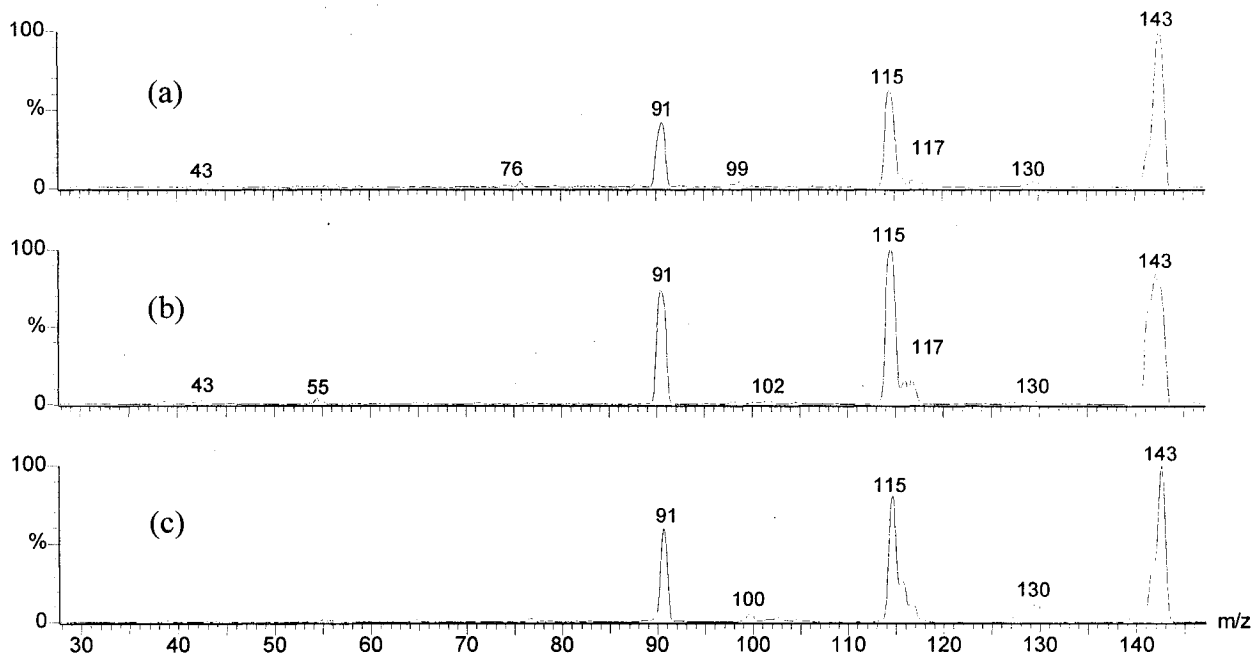

Figure 23. CID mass spectra of 2,4-dimethylquinoline (a), 2,7-dimethylquinoline (b), and Diesel *m/z* 158 (c). A collision energy of 25 eV was used for the quinolines and 30 eV for the diesel compound. Ordinate scale has been expanded.

4.3.4 Weathered Resins

To investigate the effect of environmental processes on oil, "weathered" samples of the resins were also studied by mass spectrometry. The Emergencies Science and Technology Division of Environment Canada conducts weathering experiments to simulate the physical and chemical changes that occur when oil and its products are exposed to sunlight, wind, and water [21]. The percent weathered refers to the percentage evaporative mass-loss over a 48 hour period. To determine if artificially weathered resin samples were significantly different from unweathered, we examined the number average molecular weight (Mn) for the *m/z* 220-750 regions of the crude and fuel oils and the *m/z* 75-350 region for diesel. The selection of the *m/z* range was arbitrary. This method was chosen because no significant differences were apparent through visual examination of the mass spectra for each resin sample. For each resin, the mass spectrum of three different samples was obtained and the results were averaged. The data are presented in Table 19. No weathered ASMB samples were available for our experiments.

The Mns for all the unweathered crude oil resins were in the range 367-423 Daltons. For the two fuel oils, the unweathered Mns were similar (404 and 405 Daltons) as mentioned previously, while for diesel, a Mn of 209 Daltons was obtained. With respect to weathering, we were unable to conclude whether or not this process resulted in any change in the constituents of all resins when the standard error for each was taken into account. Two possible explanations for this are that either all the components of each resin degraded equally resulting in no observable increase or decrease in Mn; or that the components lost due to weathering were not part of the

Table 19. Molecular weight statistics for weathered and unweathered resins.

Resin	% Weathered	Ave Mn	Ave S^2
ASMB	0%	395 ± 21	29 718 ± 2 346
Maui	0%	367 ± 2	34 087 ± 590
	14.12%	370 ± 3	35 768 ± 2 343
	29.76%	363 ± 7	33 522 ± 235
	43.45%	361 ± 14	35 659 ± 2 395
Tchat	0%	382 ± 5	33 527 ± 1 071
	19.4%	382 ± 3	33 537 ± 551
	38.4%	376 ± 8	32 119 ± 1 617
Alaskan Northslope	0%	393 ± 12	36 116 ± 4 250
	10%	393 ± 1	35 482 ± 1 577
	22.5%	394 ± 6	34 127 ± 800
	30.5%	393 ± 1	33 784 ± 1 089
Arabian Heavy	0%	408 ± 16	29 948 ± 929
	8.59%	411 ± 4	30 182 ± 383
	16.07%	416 ± 11	29 963 ± 509
	23.5%	417 ± 6	29 382 ± 762
Hibernia	0%	423 ± 15	30 041 ± 2 982
	10.13%	416 ± 1	31 708 ± 818
	20.8%	419 ± 3	31 116 ± 755
	35.56%	410 ± 6	32 418 ± 270
Mars	0%	414 ± 1	31 307 ± 965
	8.42%	411 ± 6	30 757 ± 938
	17.21%	413 ± 4	30 486 ± 1 374
	26.15%	415 ± 7	31 170 ± 1 178
Fuel Oil #5	0%	404 ± 4	32 003 ± 1 295
	7.25%	409 ± 1	30 206 ± 2 102
HFO 6303	0%	405 ± 9	29 928 ± 1 826
	2.5%	378 ± 30	32 665 ± 3 576
Diesel	0%	209 ± 4	6382 ± 480
	7.18%	207 ± 2	6441 ± 544
	14.20%	211 ± 7	6564 ± 120
	21.95%	212 ± 4	6465 ± 122

polar constituents which were extracted by the solvent system (acetone), and so no observable change could be measured through the mass spectra. For the fuel oils, an increase in Mn was only observed for the weathered Fuel Oil #5 and it was marginal. The breath of distribution of each resin can be seen in the variance values in Table 19. As seen in the mass spectra, the crude and fuel oil Mns have very large distributions, while a much smaller spread is observed for the diesel resins.

4.4 Conclusions

The usefulness of electrospray ionization mass spectrometry for the analysis of resin fractions of crude oil, fuel oil, and diesel has been demonstrated. Using this method, it was possible to obtain mass spectra of the polar constituents present in these resins, and use these spectra to make comparisons between the oils. Tandem mass spectra of some of the individual compounds present in ASMB crude oil helped to shed light on the unique composition of petroleum resins. The resins of this crude were found to contain carbazoles, differing by 14 mass units due to the presence of increasing alkyl substituents. The findings also showed that the resins of commercial grade fuel oils can be significantly different in their composition. The analysis of resins from a "summer diesel" showed the presence of quinoline type chemicals in this fuel mixture along with oxygen or sulphur based chemicals and alkyl carbazoles. Finally, it was shown that the effect of weathering on the composition of petroleum resins can be studied by comparing the average number molecular weights generated from the mass spectra. In this case, increases and decreases in the number average molecular weights for several resins were observed, but these were not significant when standard error was taken into account.

4.5 References

1. Rudzinski, W.E. and Aminabhavi, T.M. A review on extraction and identification of crude oil and related products using supercritical fluid technology. *Energy & Fuels* **2000**, 14, 464-475.
2. Mitra-Kirtley, S.; Mullins, O.C.; Ralston, C.Y.; Sellis, D.; Pareis, C. Determination of sulfur species in asphaltene, resin, and oil fractions of crude Oils. *Applied Spectroscopy* **1998**, 52, 1522-1525.
3. Boukir, A.; Aries, E.; Guiliano, M.; Asia, L.; Doumenq, P.; Mille, G. Subfractionation, characterization and photooxidation of crude oil resins. *Chemosphere* **2001**, 43, 279-286.
4. Khadim, M.; Sarbar, M. Role of asphaltene and resin in oil field emulsions. *J. Petrol. Sci. Eng.* **1999**, 23, 213-221.
5. Christy, A.; Dahl, B.; Kvalheim, M. Structural features of resins, asphaltenes and kerogen studied by diffuse reflectance infrared spectroscopy. *Fuel* **1989**, 69, 430-435.
6. Ali, M.F.; Bukhari, A.; Hasan, M. Structural characterization of arabian heavy crude oil residue. *Fuel Sci. Technol. Int.* **1989**, 7, 1179-1208.
7. Khattab, S.A.; El-Azzaby, O.H. Abo-lemon, F.S.; Roushdy, M.I. Investigation of the chemical composition of oils, resins, and asphaltenes of Jalo Libyan crude oil by NMR spectroscopy. *Egypt. J. Chem.* **1978**, 21, 421-430.
8. Buchanan, M. Mass spectral characterization of nitrogen-containing compounds with ammonia chemical ionization. *Anal. Chem.* **1982**, 54 (3), 571-574.
9. Pearson, C.; Gharfeh, S. Automated high-performance liquid chromatography determination

of hydrocarbon types in crude oil residues using a flame ionization detector. *Anal. Chem.* **1986**, 58, 307-311.

10. Zhan, D., and Fenn, J.B. Electrospray mass spectrometry of fossil fuels. *Int J Mass Spectrom.* **2000**, 194, 197-208.
11. Roussis, S.; Proulx, R. Molecular weight distributions of heavy aromatic petroleum fractions by Ag^+ electrospray ionization mass spectrometry. *Anal. Chem.* **2002**, 74, 1408-1414.
12. Roussis, S.G; Fedora, J.W. Quantitative determination of polar and ionic compounds in petroleum fractions by atmospheric chemical ionization and electrospray mass spectrometry. *Rapid Commun. M. Spec.* **2002**, 16, 1295-1303.
13. Rodgers, R.; Hendrickson, C.; Emmett, M.; Marshall, A.; Greaney, M.; Qian, K. Molecular characterization of petroporphyrins in crude oil by electrospray ionization Fourier transform ion cyclotron resonance mass spectrometry. *Can. J. Chem.* **2001**, 79, 546-551.
14. Qian, K.; Robbins, W.; Hughey, C.; Cooper, H.; Rodgers, R.; Marshall, A. Resolution and identification of elemental compositions for more than 3000 crude acids in heavy petroleum by negative-ion microelectrospray high-field Fourier transform ion cyclotron resonance mass spectrometry. *Energy Fuels* **2001**, 15, 1505-1511.
15. Gough, M. A.; Langley, G. J. Analysis of oilfield chemicals by electrospray-mass spectrometry. *Rapid Commun. M. Spec.* **1999**, 13, 227-236.
16. McCormack, P.; Jones, P.; Rowland, S. J. Liquid chromatography/electrospray ionisation mass spectrometric investigations of imidazoline corrosion inhibitors in crude oils. *Rapid Commun. M. Spec.* **2002**, 16, 705-712.
17. Emergencies Science and Technology Division, Environment Canada. Draft method for the

determination of the hydrocarbon group constituents of oil and petroleum products. January, **2002**.

18. Busch, K. L.; Glish, G. L.; McLuckey, S. A. *Mass Spectrometry/Mass Spectrometry*; VCH Publishers: New York, **1988**.
19. Willsch, H.; Clegg, H.; Horsfield, B.; Radke, M.; Wilkes, H. Liquid chromatographic separation of sediment, rock, and coal extracts and crude oil into compound classes. *Anal. Chem.* **1997**, 69, 4203-4209.
20. Ignatiadis, I.; Schmitter, J.; Arpino, P. Separation and identification by gas chromatography and gas-chromatography-mass spectrometry of the nitrogen compounds from a deasphalted heavy oil. Evolution of their distribution after a catalytic hydrotreatment. *J. Chromatogr.* **1985**, 324, 87-111.
21. Emergencies Science and Technology Division, Environment Canada. Draft method for the simulated weathering of oil and petroleum products. January, **2002**.

Claim to Original Research

I certify that this thesis does not incorporate without acknowledgment any material previously submitted for a degree or diploma in any university. Further, to the best of my knowledge and belief it does not contain any material previously published or written by another person except where reference is made in the text.

The research presented here involves the study of the resin fraction of several petroleum mixtures using electrospray ionization mass spectrometry, an accomplishment that at the time of this writing has not appeared in any scientific publication or otherwise. Other researchers have used ESI to study various fossil fuels and fuel additives but have not employed it for the study of resin fractions. The use of tandem mass spectrometry for the characterization and identification of the constituents present in petroleum resins is also a new technique. This method may prove useful for tracing the origin of petroleum products during investigations of oil spills in water or on land. The results presented here also demonstrate that tandem ESI can be used to distinguish isomeric nitrogen containing chemicals using relative intensity alone. This may be useful not only for the study of polar chemicals in petroleum, but also for chemicals present in any aqueous environmental matrix. Lastly, the use of ESI in the manner presented here to study the effect of weathering on petroleum samples is also an original concept that has not appeared in the scientific literature. Traditionally, the weathering of crude oils has been studied by means of GC-MS as discussed earlier. It is hoped that the method presented here may be employed by others and further developed so as to become a common technique for this type of analysis.